1. Report No.	2. Government Accession No.	3. Recipient's Catalog No.

4. Title and Subtitle	5. Report Date
Development Of A Wideband Pulse Quaternary Modulation System	May 1974
	6. Performing Organization Code
7. Author(s) J. A. Federhofer, et. al	8. Performing Organization Report No.
9. Performing Organization Name and Address McDonnell Douglas Astronautics Company-East Box 516 St. Louis, Mo. 63166	10. Work Unit No.
	11. Contract or Grant No. NAS5-23248
12. Sponsoring Agency Name and Address Goddard Space Flight Center Greenbelt, Maryland 20771 Attn: M. Fitzmaurice Code 524	13. Type of Report and Period Covered Final Report 28 June 1973- 28 January 1974
	14. Sponsoring Agency Code

15. Supplementary Notes

16. Abstract

The objective of this program was to provide laboratory data to verify the Pulse Quaternary Modulation (PQM) theoretical predictions.

During this program the first laboratory PQM laser communication system was successfully fabricated, integrated, tested and demonstrated.

System bit error rate tests were performed and, in general, indicated approximately a 2 dB degradation from the theoretically predicted results. These tests thus indicated that no gross errors were made in the initial theoretical analysis of PQM. The relative ease with which the entire PQM laboratory system was integrated and tested indicates that PQM is a viable candidate modulation scheme for an operational 400 Mbps baseband laser communication system.

(NASA-CR-139129) DEVELOPMENT OF A WIDEBAND PULSE QUATERNARY MODULATION SYSTEM Final Report, 28 Jun. 1973 - 28 Jan. (McDonnell-Douglas Astronautics Co.) 54 p HC $4.25 CSCL 17B G3/32 53702

N75-10288

Unclas

17. Key Words (Selected by Author(s))	18. Distribution Statement
Laser Communications Baseband Modulation Pulse Quaternary Modulation	

19. Security Classif. (of this report)	20. Security Classif. (of this page)	21. No. of Pages	22. Price*
Unclassified	Unclassified	60	

*For sale by the Clearinghouse for Federal Scientific and Technical Information, Springfield, Virginia 22151.

NOV 1974
RECEIVED
NASA STI FACILITY
INPUT BRANCH

THIS PAGE INTENTIONALLY LEFT BLANK

PREFACE

This report was prepared by the McDonnell Douglas Astronautics Company-East, McDonnell Douglas Corporation, St. Louis, Missouri, under contract NAS5-23248, Development of a Wideband Pulse Quaternary Modulation System. This report covers the period from 28 June 1973 through 28 January 1974 and is the final report of this contract.

The work described herein was carried out by the Advanced Electronic Techniques Department at the McDonnell Douglas Astronautics Company-East, Box 516, St. Louis, Missouri 63166.

The Project Engineer was J. A. Federhofer. Other contributors to the program were L. B. Allen, J. J. Becker, J. P. Brand, J. S. Brookman, A. J. Chenoweth, R. B. Fluchel, S. I. Green, G. M. Lee, D. D. Meyer, V. H. Nettle, S. F. Pursley, F. J. Richterkessing, and J. R. Teague. The program received technical direction from A. L. Furfine (Department Manager), R. A. Stacy (Branch Manager), and M. Ross (Manager, Laser Communications) in the MDAC organization. J. A. Callahan coordinated artwork and reports.

PRECEDING PAGE BLANK NOT FILMED

THIS PAGE INTENTIONALLY LEFT BLANK

TABLE OF CONTENTS

PRECEDING PAGE BLANK NOT FILMED

ILLUSTRATIONS

ILLUSTRATIONS

(cont'd)

THIS PAGE INTENTIONALLY LEFT BLANK

1. INTRODUCTION

In 1971, McDonnell Douglas Astronautics Company-East (MDAC-E) conceived a modulation format using mode-locked lasers for a digital baseband space laser communications system which we denote as Pulse Quaternary Modulation (PQM)*. PQM is an M-ary modulation format which theoretically achieves a 5 dB to 6 dB improvement over the Pulse Gated Binary Modulation (PGBM) format. In PQM, information is contained in both time position and polarization. Two possible time positions are utilized along with two orthogonal polarizations. Thus each laser pulse transmitted has the ability of being encoded in one of four possible states.

The objective of this program was to provide laboratory data to verify the theoretical predictions for the PQM format. During this program, MDAC-E assembled and tested the electronic modules necessary to implement the PQM format, refurbished available breadboard electrooptic components, and integrated GFE and MDAC-E components into a breadboard 400 Mbps PQM laser communication system. The system was evaluated for bit error rate performance and the results compared to similar test results obtained for PGBM during contracts NAS5-11471 and NAS5-11474.

*Patent Applied For.

THIS PAGE INTENTIONALLY LEFT BLANK

2. PERFORMANCE SUMMARY

The general results of the system bit error rate (BER) tests verified the PQM theory. Figure 1 shows a direct comparison of PQM results obtained during this program and PGBM results obtained during NASA contracts NAS5-11471 and NAS5-11474. The two experimental curves, for a modulator extinction ratio of 10 to 1, are plotted as Bit Error Probability versus Mean Signal Photoelectrons Per Bit referred to the transmitter laser output. This referral assumes a quantum efficiency of 100% for the receiver photodetectors and no optical losses. This type of referral is necessary, when comparing the relative advantages of PQM over PGBM, in order that the true advantage appears on the comparison graph. Referring to Figure 1 it is seen that the two experimental curves differ by 6.8 dB at 10^{-6} bit error rate. This discrepancy can be explained by noting that the PGBM data obtained during NASA contracts NAS5-11471 and NAS5-11474 did not approach theoretical predictions as close as the PQM data obtained during this contract.

Figure 2 shows a comparison of PQM bit error rates with background levels of $N_bG = 0$ and $N_bG = 1.20$ pe. N_b is equal to the background photoelectrons per nanosecond and G is the effective DCFP gate width in nanoseconds. From Figure 2 it is seen that the experimental results with $N_bG = 0$ are 2.05 dB from theoretical at 10^{-6} bit error rate and the experimental results for $N_bG = 1.20$ are 1.76 dB from theoretical at 10^{-6} bit error rate. The extinction ratio for both cases is 20 to 1. The results shown on Figure 2 summarize the best results obtained during the experimental portion of this contract.

PRECEDING PAGE BLANK NOT FILMED

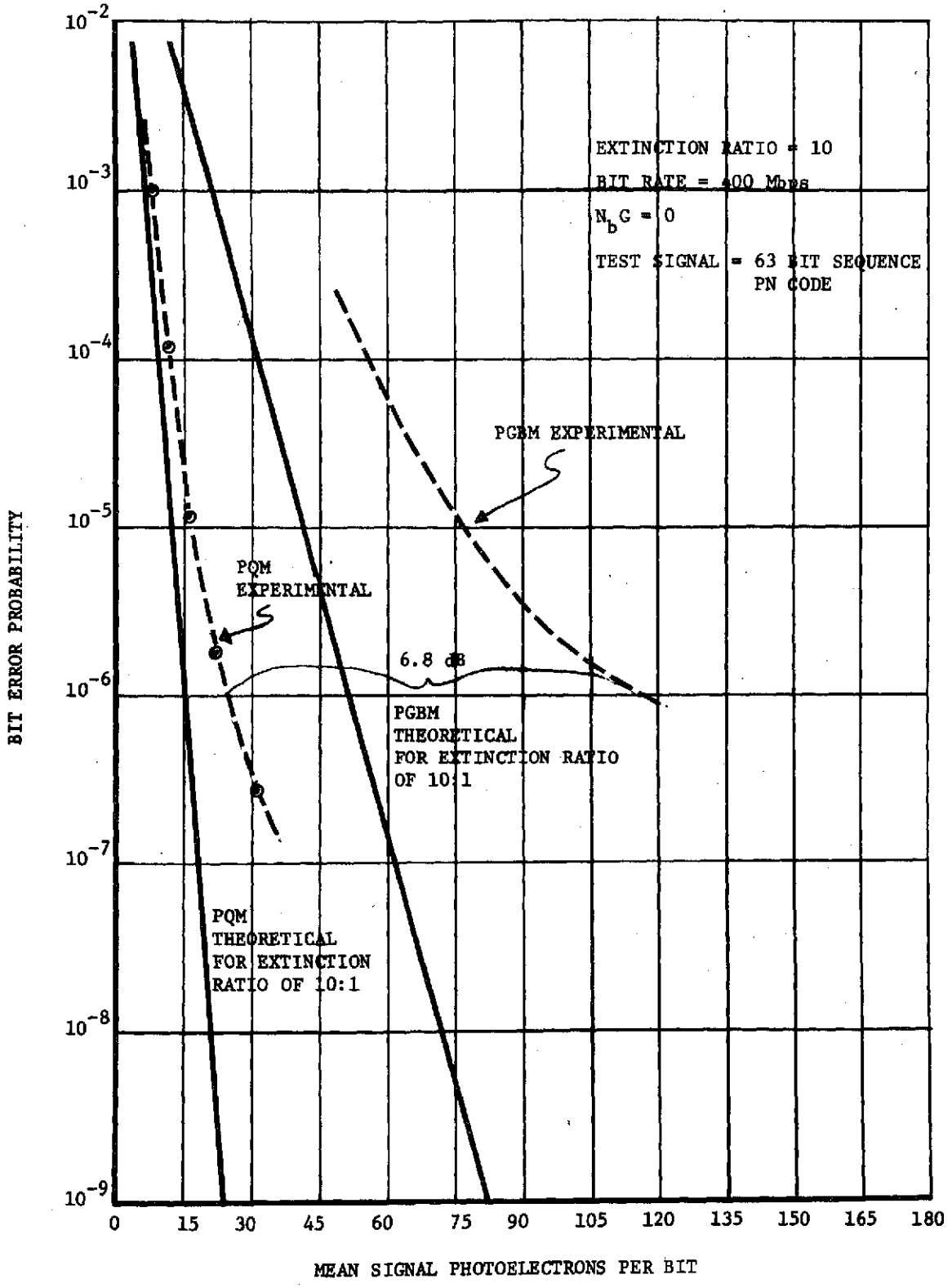

FIGURE 1 COMPARISON OF PQM AND PGBM MODULATION FORMATS

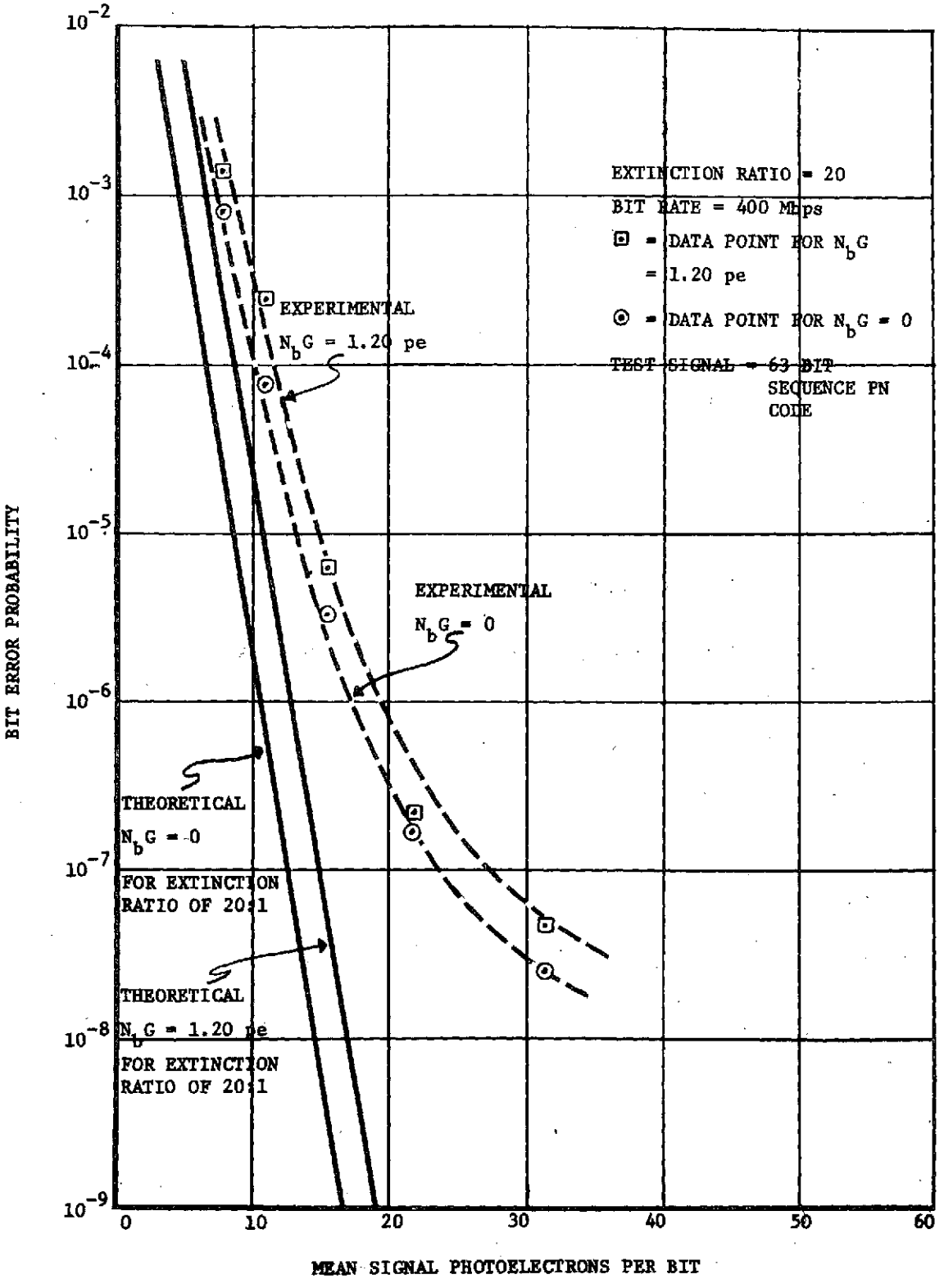

FIGURE 2 PQM BIT ERROR PROBABILITY AS A FUNCTION OF RECEIVED PHOTOELECTRONS PER BIT

THIS PAGE INTENTIONALLY LEFT BLANK

3. SYSTEM DESCRIPTION

Figure 3 shows a block diagram of the wideband PQM system. The blocks are coded to indicate the sources of each hardware element in the system.

3.1 THEORY OF OPERATION AND SYSTEM IMPLEMENTATION. In PQM, two bits of data are encoded on each laser pulse available. Two bits of data can generate four possible words (00, 01, 10, 11). For each of these words there must be a unique detectable situation. In the wideband PQM system, pulse polarization and pulse time position are used to uniquely determine the correct two bit word. Let B_1 and B_2 represent the first and second bit of the two bit words. Also let B_1 and B_2 be applied to modulator 1 and modulator 2 respectively. Assume the modulators are biased such that a binary "1" causes the modulator to change the polarization of the input pulses and a binary "0" causes the modulator to pass the pulses unchanged in polarization. The polarizing time delay at the output of modulator 1 can be arranged such that vertically polarized pulses are delayed and horizontally polarized pulses are undelayed. The laser pulse output is assumed to be horizontally polarized. Horizontally polarized pulses are designated S_1 and vertically polarized pulses, S_2. A second subscript is added to indicate time slot 1 (undelayed pulse) or time slot 2 (delayed pulse). Making use of the above information and Figure 3 the following truth table can be generated for a transmitted signal.

	B_1B_2
S_{11}	0 0
S_{21}	0 1
S_{22}	1 0
S_{12}	1 1

The PQM receiver has two functions to accomplish in the detection process. It must determine the polarization and time position of each pulse sent. Polarization separation is accomplished by a polarizing beamsplitter positioned at the receiver input. The PQM demodulation electronics

PRECEDING PAGE BLANK NOT FILMED

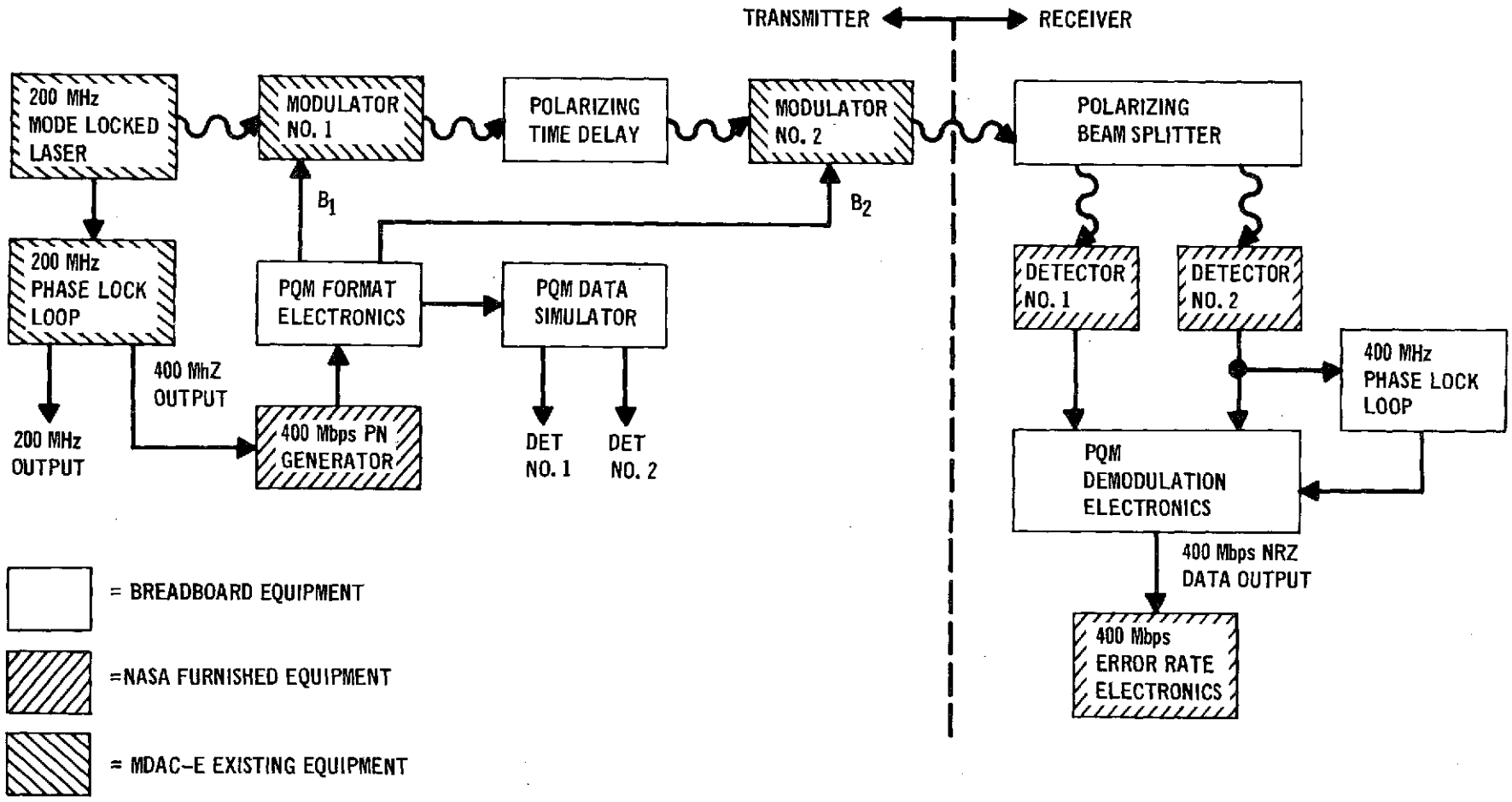

FIGURE 3 WIDEBAND PQM SYSTEM
Block Diagram

determine which detector has received the pulse and which time position the pulse occupies. It then uses this information to reconstruct the original transmitted signal.

3.1.1 Breadboard Equipment. Referring to Figure 3 the equipment which were breadboarded for this contract are:

1. PQM Format Electronics
2. PQM Data Simulator
3. Polarizing Time Delay and Beam Splitter
4. 400 MHz Phase Locked Loop
5. PQM Demodulation Electronics

The PQM Demodulation Electronics are further subdivided into four subsystems:

a) PQM Receiver Preamplifier Module
b) PQM Decision Module
c) PQM Receiver Multiplexer Module
d) PQM Ambiguity Resolver

3.1.2 PQM Format Electronics. Figure 4 is a logic diagram of the PQM Format Electronics. The 400 Mbps NRZ data to be transmitted is demultiplexed by the format electronics into two 200 Mbps NRZ data streams. These two data streams are used as the inputs to the two PQM modulators. Their compliments are used as inputs to the PQM data simulator. The format electronics also supplies a 200 Mpps pulse train to the data simulator module. Three 500 MHz MECL III flip-flops and discrete transistor circuits were used to implement the PQM Format Electronics. The wider bandwidths available with the discrete circuits were required at key positions throughout the electronics.

3.1.3 PQM Data Simulator. Figure 5 is a logic diagram of the PQM Data Simulator. The PQM Data Simulator was used to run system tests on the electronics without the use of the system optical components. The outputs of the PQM Data Simulator simulate the receiver optical detector outputs minus noise. By adding Gaussian noise to the

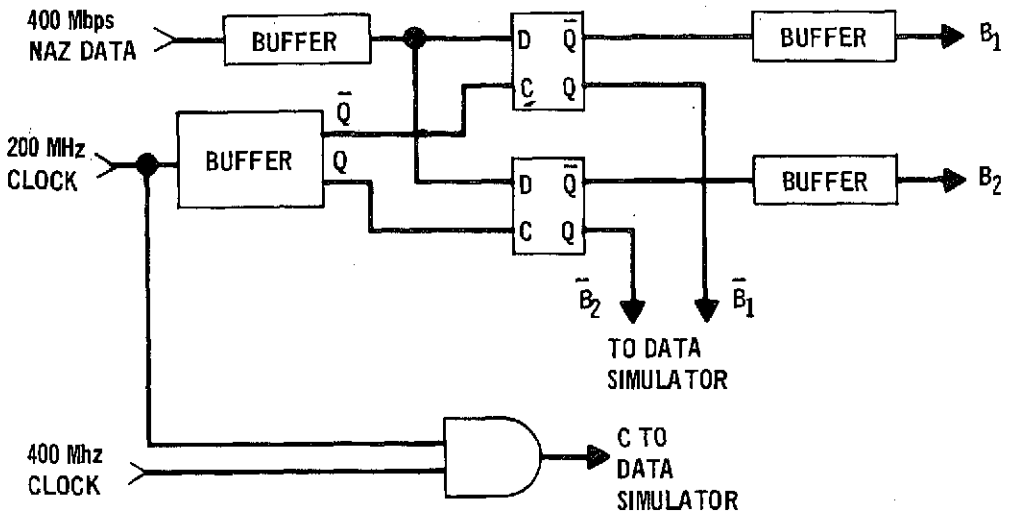

FIGURE 4 PQM FORMAT ELECTRONICS

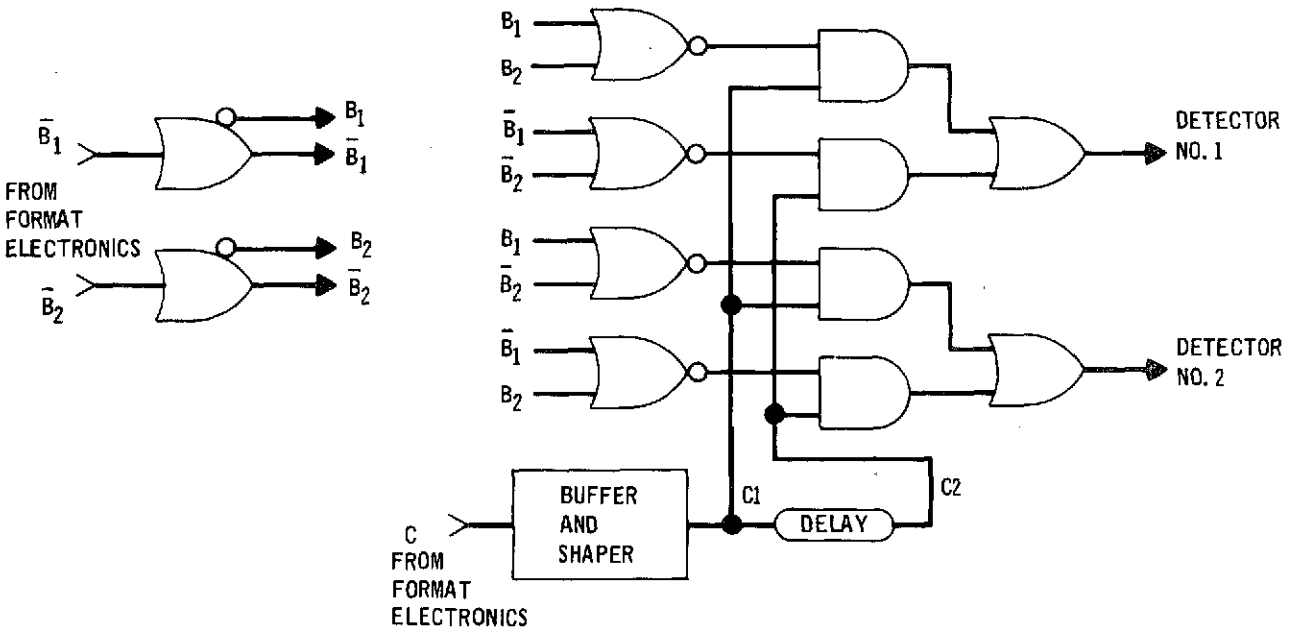

FIGURE 5 PQM DATA SIMULATOR

simulated outputs the PQM electronics were checked under a signal plus noise condition. No provisions for adding noise to the simulated data were incorporated in the simulator module. Simulated data with noise was obtained by attenuating the simulated signal and passing it through amplifiers such that the amplifier noise becomes an appreciable factor. The signal-to-noise ratio was adjusted by changing the attenuation. It should be pointed out that noise obtained in this manner in Gaussian as compared to Poisson noise in the actual optical system. The type of noise present in the simulated data source was not important because the simulated source was used only for initial alignment of the electronic components in the system. Referring to Figure 5, if C_1 is the undelayed clock and C_2 the delayed clock, the following logical equations describe the operation of the data simulator.

$$C_1 (\bar{B}_1\bar{B}_2) + C_2 (B_1B_2) = S_{11} + S_{12}$$

$$C_1 (B_1\bar{B}_2) + C_2 (B_1\bar{B}_2) = S_{21} + S_{22}$$

These equations are derived from the truth table given in Section 3.1.

The PQM Data Simulator was implemented using MECL III integrated logic circuits and logic circuits implemented with discrete transistors. Referring to Figure 5, the "nor" gates and "or/nor" gates were implemented with MECL III circuits and the remainder of the simulator was implemented with discrete transistor circuits. The initial design used the MMT 3960 transistor with an f_t of 2.25 GHz. Figure 6 shows output waveforms of the initial design. The pulse widths are 1.0 to 1.5 ns with nonuniform amplitudes. These outputs were unacceptable and it was decided that the simulator had to be redesigned. The MMT 8015 transistor with an f_t of 4.5 GHz was used as the basic element in the discretely implemented circuits for the redesigned simulator. In the redesign, additional shaping networks were added at each simulated output to obtain uniform pulse shape and amplitude. These

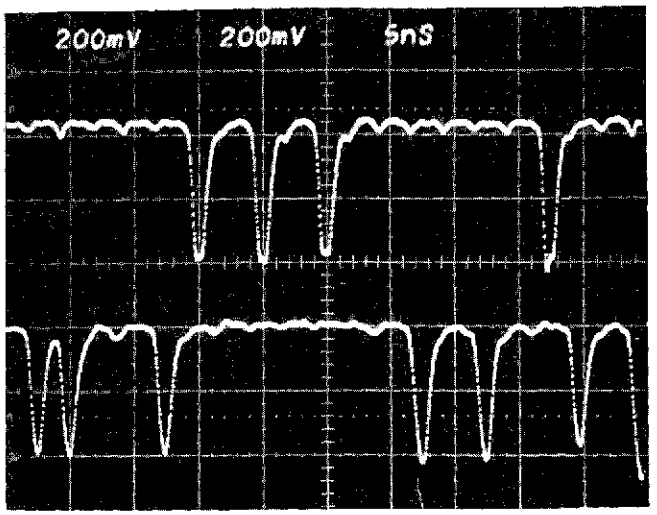

P_2 Output

P_1 Output

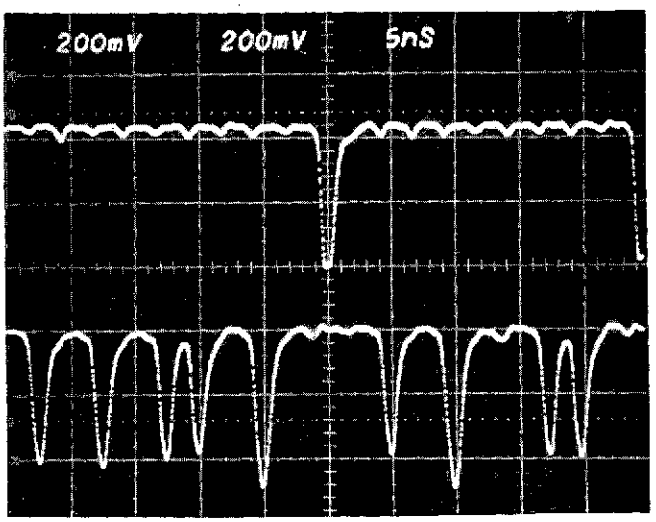

P_2 Output

P_1 Output

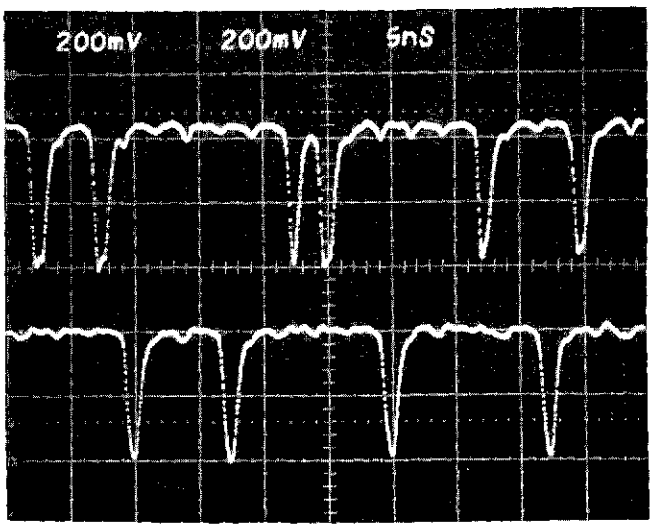

P_2 Output

P_1 Output

FIGURE 6 DATA SIMULATOR OUTPUTS

REPRODUCIBILITY OF THE
ORIGINAL PAGE IS POOR

networks each consist of three cascaded HP23 transistor emitter coupled pairs. These transistors have current gain-bandwidths of 4.0 GHz and low package parasitics which provide 150 ps switching times. Figure 7 shows the simulated output for various portions of the 63 bit PN sequence. Figure 8 shows the simulated output with increased time scale sensitivities. The pulses are 500 ps wide at the base and have 180 to 200 ps risetimes.

3.1.4 Polarizing Time Delay and Beam Splitter. The major passive optical components used in the PQM breadboard system were the transmitter polarizing time delay and the receiver polarizing beam splitter. A functional diagram of the polarizing time delay unit is shown in Figure 9. The light entering the polarizing time delay unit is analyzed by the first polarizing beamsplitter prism. The horizontal polarized light S_1 passes through both this prism and the second polarizing beamsplitter prism. The vertically polarized light S_2 is reflected out at right angles to the incoming light. This light is then returned parallel to its outgoing path by the right angle prism. It then enters the second polarizing beam-splitter prism which reflects it collinear with the horizontally polarized beam. The length of the time delay is set precisely to 2.5 ns by adjusting the spacing between the right angle beam prism and the polarizing beam splitter prisms. Glass slides were used as optical attenuators in the S_1 path to compensate for additional losses in the S_2 path. They were placed between the two polarizing beam splitter prisms. The difference in the losses between the S_1 path and the S_2 path was measured at 3% to 4%. There was no attempt made to optimize the polarizing time delay unit for optical losses.

A polarizing beamsplitter prism of the type used in the time delay unit is used at the receiver for splitting the two polarizations, one into each DCFP detector. One or the other of the two detectors receives every laser pulse transmitted by the laser. In PQM laser pulses of both polarizations are transmitted whereas, in PGBM, only pulses of one polarization are transmitted.

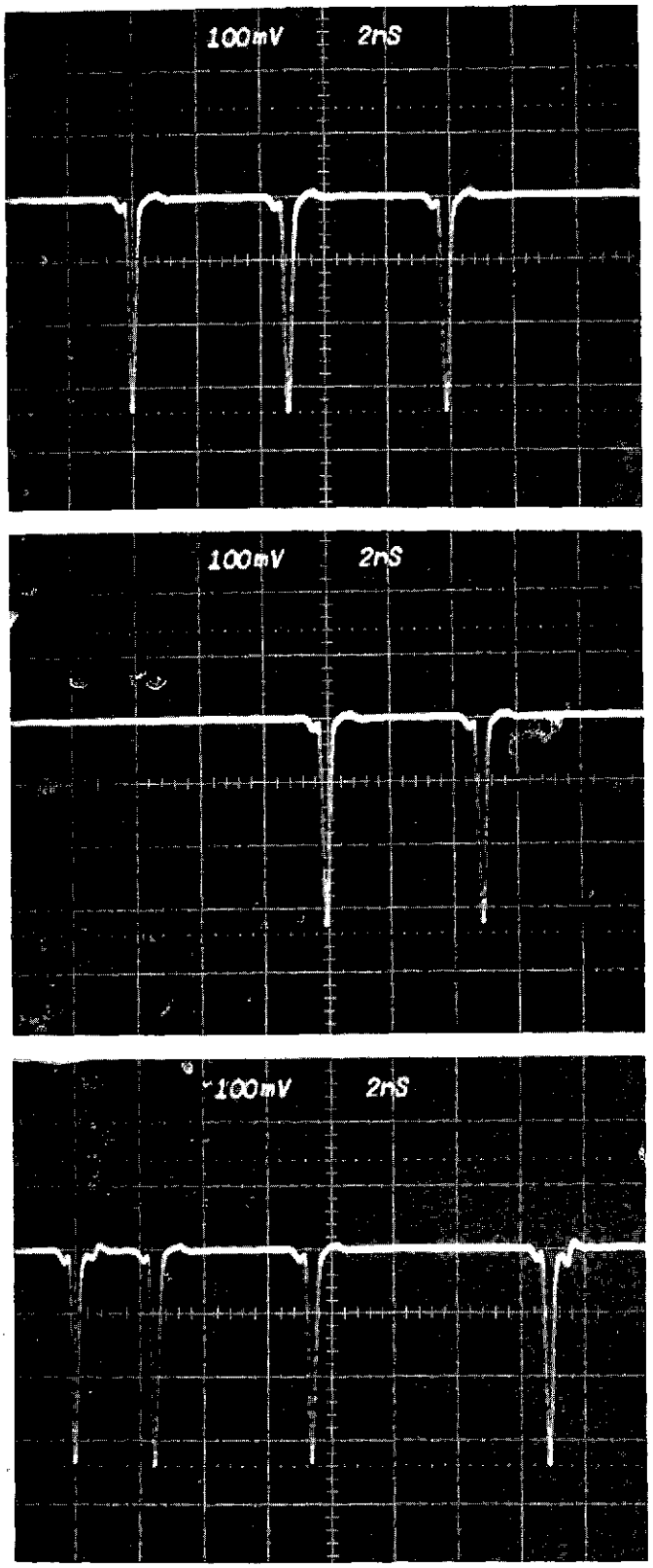

Photos taken with Output of Simulator Directly into a 25 ps Sampling Head.

FIGURE 7 PQM DATA SIMULATOR WAVEFORMS

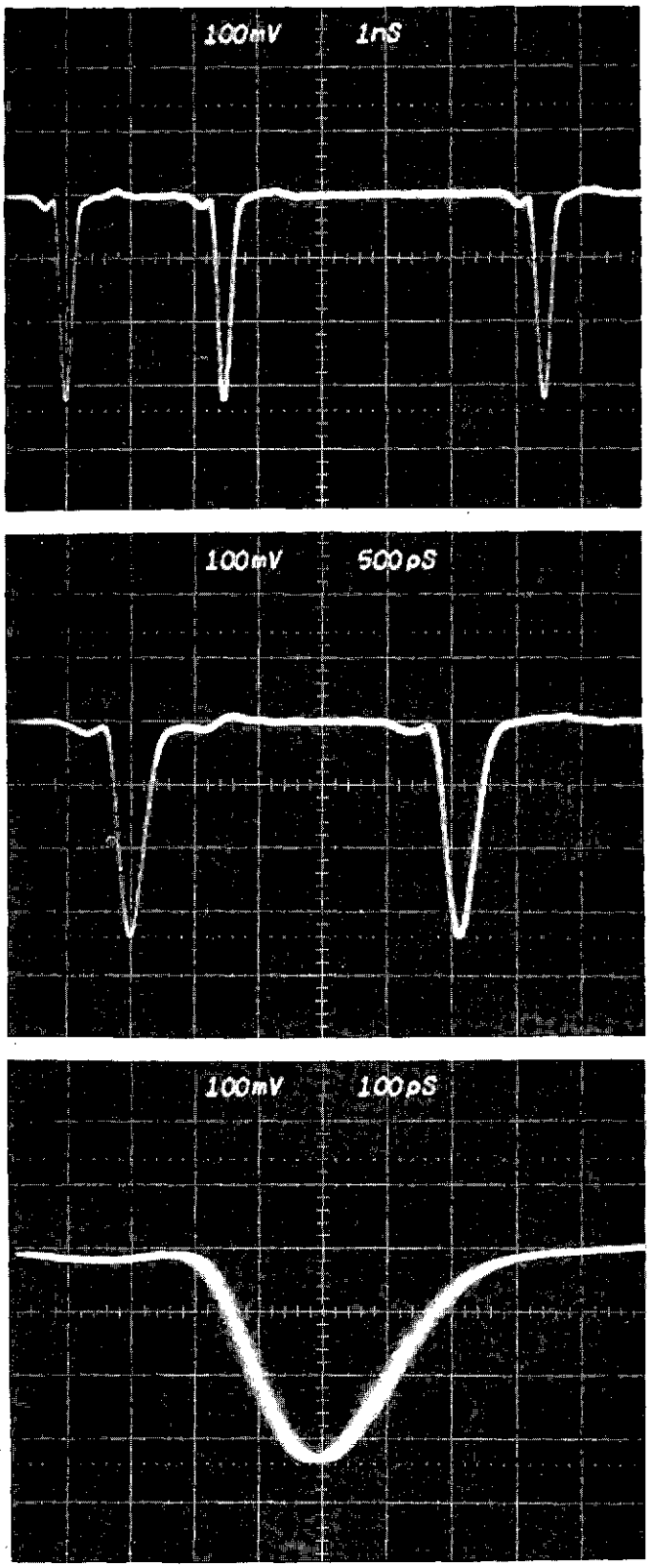

Photos taken with Output of Simulator Directly into a 25 ps Sampling Head.

REPRODUCIBILITY OF THE ORIGINAL PAGE IS POOR

FIGURE 8 PQM DATA SIMULATOR WAVEFORMS

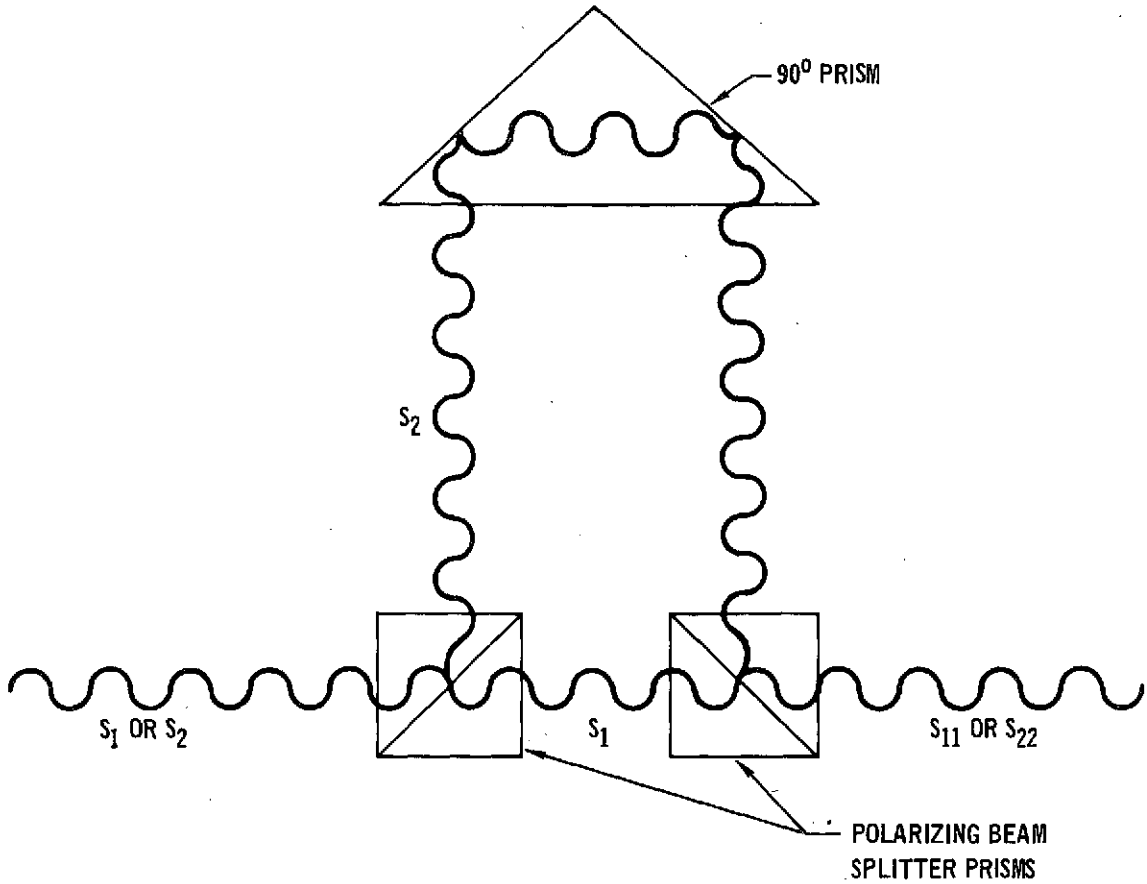

FIGURE 9 POLARIZING TIME DELAY

3.1.5 PQM Demodulation Electronics. The demodulation electronics must make the proper decisions to determine the position of the received pulses so that it can reconstruct the transmitted signal. Figure 10 is a block diagram of the PQM Demodulation Electronics. Each of the output signals from the two photomultipliers are amplified with low noise wideband amplifiers. The output of each amplifier is split into three paths. One path from each amplifier goes directly to the 1 of 4 detector. A second path from each amplifier is delayed by 1/2 word period and then goes to the 1 of 4 detector. The third path from one of the amplifiers after being filtered and amplified is used as the input to the receiver 400 MHz Phase Locked Loop. The third path from the other amplifier is used as a reference for the ambiguity resolver. The 1 of 4 detector is clocked at a 200 MHz rate. Its output is latched after clocking until the next clock

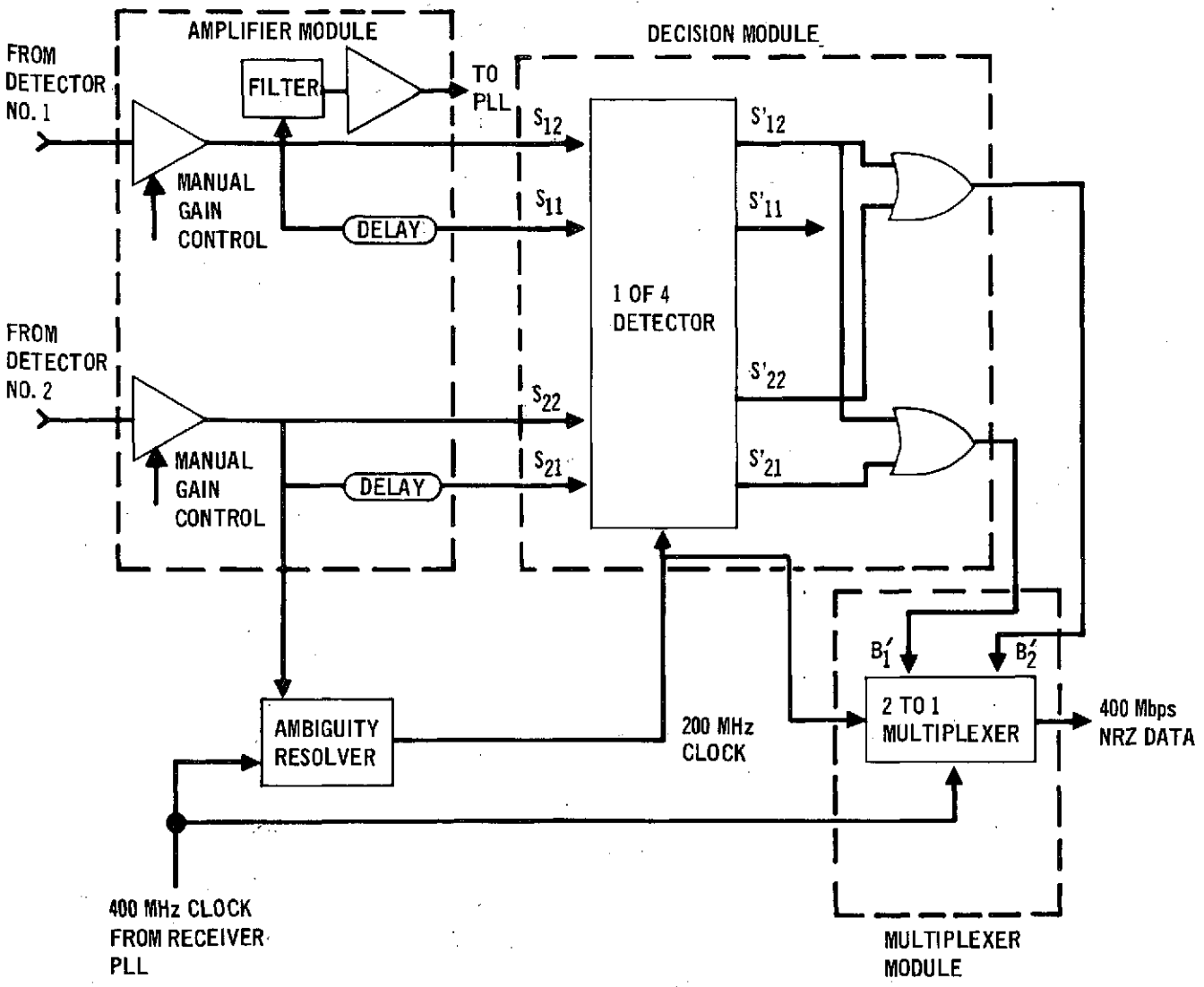

FIGURE 10 PQM DEMODULATION ELECTRONICS

pulse appears at which time a new decision is made. The 200 MHz clock is time aligned with the input signals to coincide with the expected time of arrival of the nondelayed and delayed pulses for a given word period as shown in Figure 11. Figure 11 is a timing diagram showing the decision process for a representative signal. The output of the 1 of 4 detector is decoded and used to reconstruct the two 200 Mbps data streams present at the modulator inputs. The multiplexer module multiplexes the two 200 Mbps data streams into one 400 Mbps data stream, thus reconstructing the data originally entered into the format electronics.

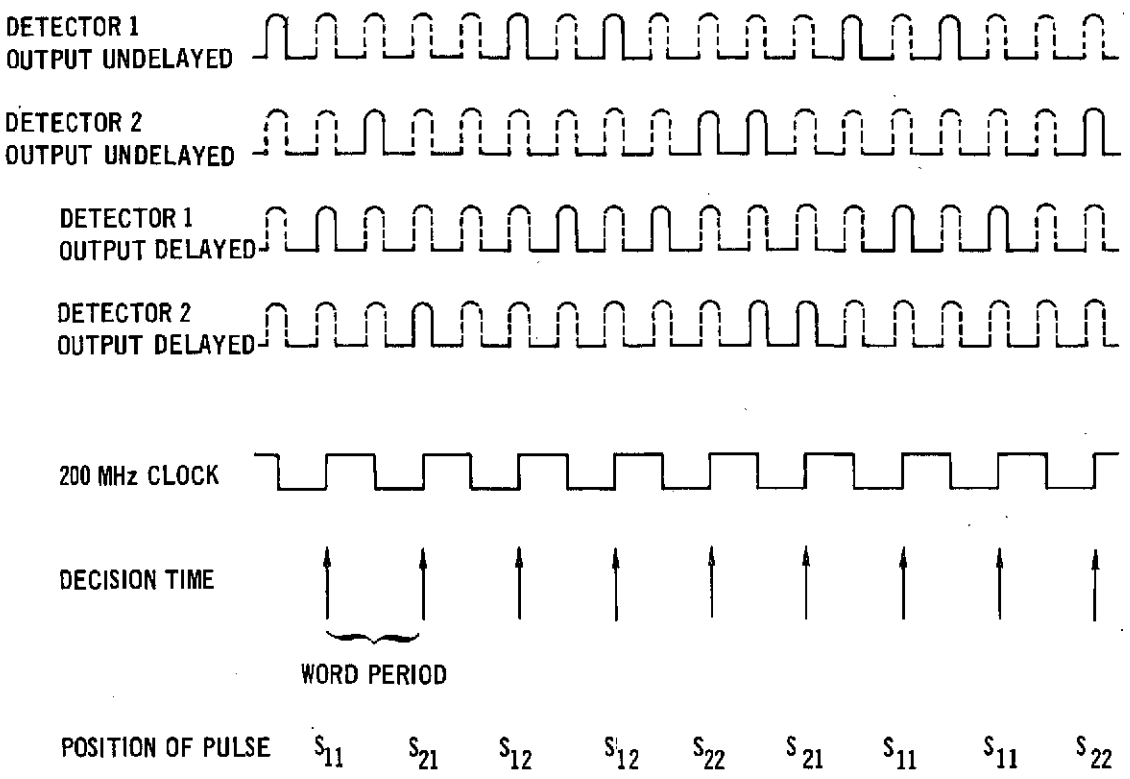

FIGURE 11 DECISION PROCESS TIMING DIAGRAM

The receiver decision process occurs at a 200 MHz rate. Thus a 200 MHz clock is needed at the receiver. Various studies of the PQM spectral content show that the 200 MHz component is highly dependent on the information content of the transmitted message and disappears completely when the probabilities of ones and and zeros are equal. Figure 12 shows the power spectrum of one of the outputs of the PQM Data Simulator for a 63 bit sequence PN code. The 200 MHz line for this case is seen to be more than 30 dB down from the 400 MHz line. Thus the recovery of the 200 MHz component directly from the received signal is not practical. The 400 MHz component does not have this data dependent behavior and is readily recovered with a Phase Locked Loop. When this 400 MHz signal is divided by two, in order to be used as the receiver clock, it has a 180° phase ambiguity. The receiver ambiguity resolver utilizes a nonlinear element to reinstate a a 200 MHz component in the received data. It then compares the

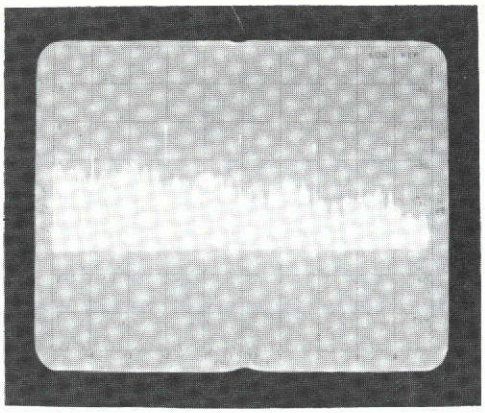

(a) 800 MHz at center
200 MHz/div

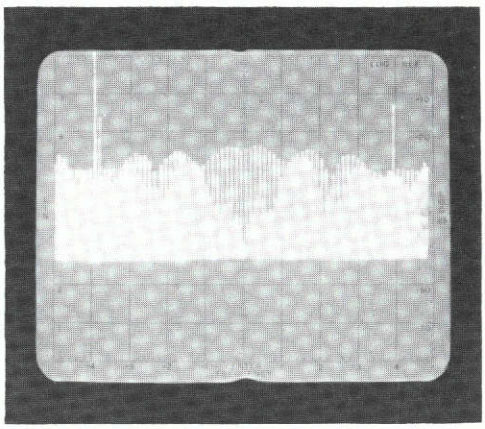

(b) 200 MHz at center
50 MHz/div.

REPRODUCIBILITY OF THE
ORIGINAL PAGE IS POOR

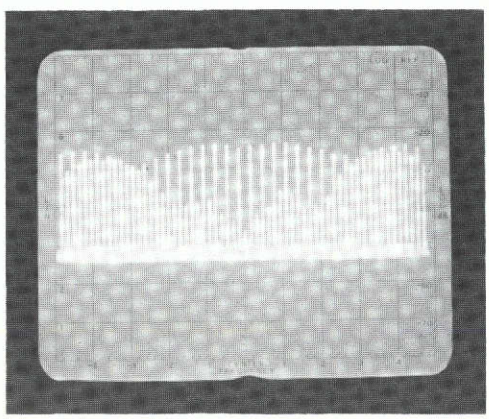

(c) 200 MHz at center
20 MHz/div

FIGURE 12 POWER SPECTRUM OF PQM SIMULATED SIGNAL

phase of this component with the phase of the 200 MHz clock and produces a correction voltage that allows the ambiguity to be resolved. Each of the four modules composing the PQM demodulation electronics will now be explained in detail.

PQM Receiver Preamplifier Module

Low noise wideband preamplifiers are required at the outputs of each of the photomultipliers to increase the signal level to a point that is usable by the receiver electronics. Figure 13 is a block diagram of the preamplifier module. The amplifiers used in the signal paths are HP35002 postage stamp amplifiers. Each of these amplifiers has 20 dB gain and a bandwidth of 700 MHz. Each signal path utilizes two of these amplifiers in cascade giving an overall possible gain of 40 dB and a bandwidth of approximately 500 MHz. The minimum bandwidth required to prevent intersymbol interference is 408 MHz. This number was derived using first order approximations and the following assumptions:

1. Photodetector output pulses are rectangular and are 700 ps wide.
2. No more than 1% residue from pulse to pulse is permissable.

The residue from any pulse is given by

$$E_R = E_0 \, e^{-t_m 2\pi B}$$

where

E_R = pulse residue
E_0 = pulse amplitude
B = 3 dB bandwidth
t_m = time measured from end of pulse

For 1% residue we have

$$0.01 = e^{-t_m 2\pi B}$$

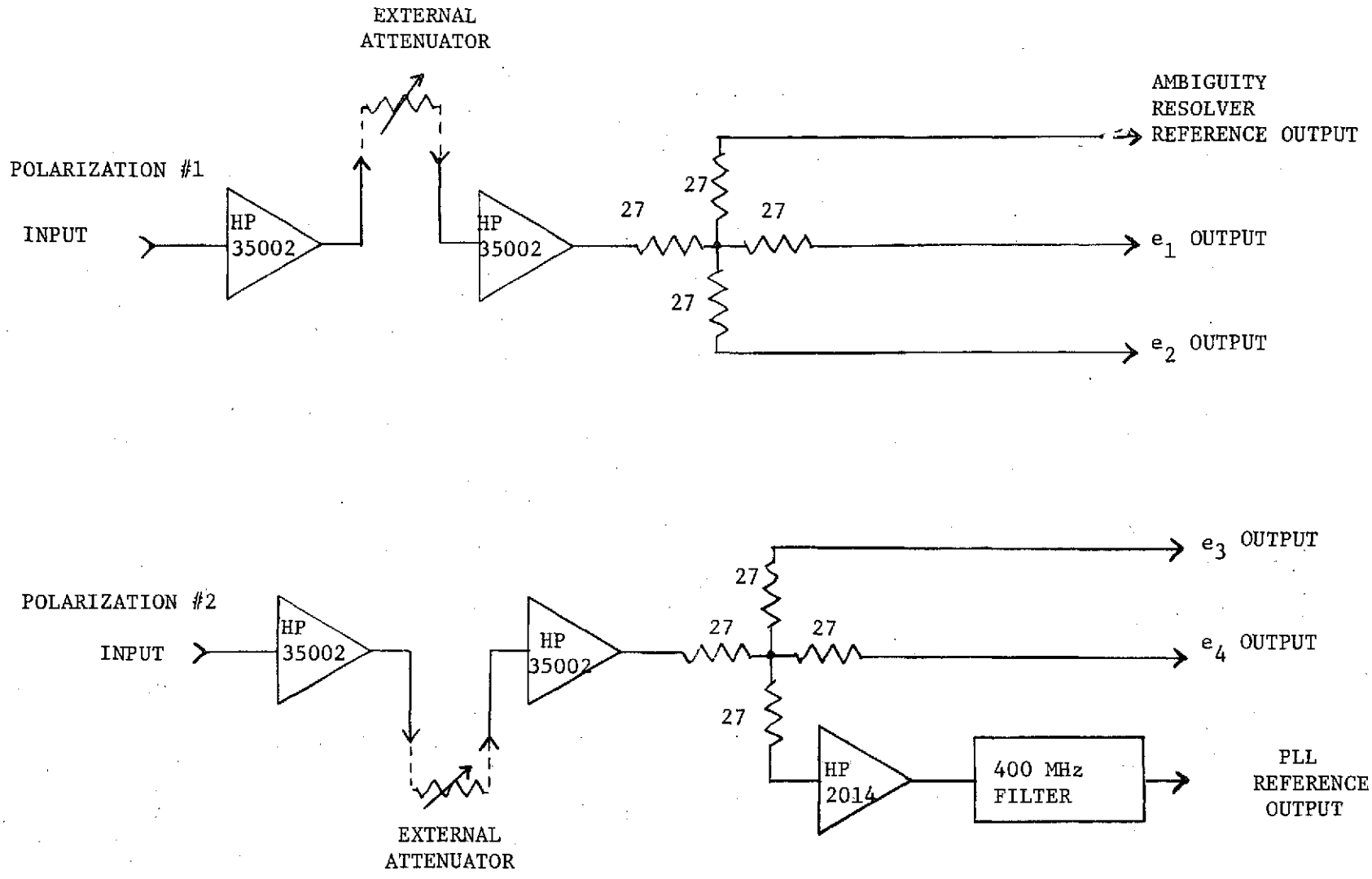

FIGURE 13 400 Mbps PQM AMPLIFIER MODULE

or

$$B = \frac{4.61}{2\pi t_m}$$

Using the above equation the minimum bandwidth can be calculated by letting

B = minimum required bandwidth

t_m = minimum time between any two pulses

If we assume 700 ps pulse widths t_m becomes 1.8 ns for 400 Mbps PQM. Thus

$$B = \frac{4.61}{(2\pi)\ (1.8 \times 10^{-9})} = 408 \text{ MHz}$$

By reducing the bandwidth of our preamplifiers to this minimum required bandwidth we could theoretically improve our signal-to-noise ratio and thus obtain better results. From past experience we know that the 500 MHz amplifier bandwidth is close enough to the theoretical minimum such that no significant benefits would be obtained by further limiting. The low frequency cutoff of the amplifiers is approximately 100 kHz.

The preamplifier noise figure for the cascaded pair was measured to be less than 5 dB in each of the signal paths. This figure was well below that required, such that preamplifier noise did not enter into the error source of the system.

The external attenuators were added between the cascaded amplifiers to allow a wide range of input signal levels and to compensate for any gain mismatch in the photomultipliers or wideband amplifiers.

PQM Decision Module

The PQM decision module must decide in which one of four possible positions the signal pulse appears for each PQM word period. It must then decode the decision and reconstruct two 200 Mbps data streams representing the inputs to the PQM modulators. Figure 14

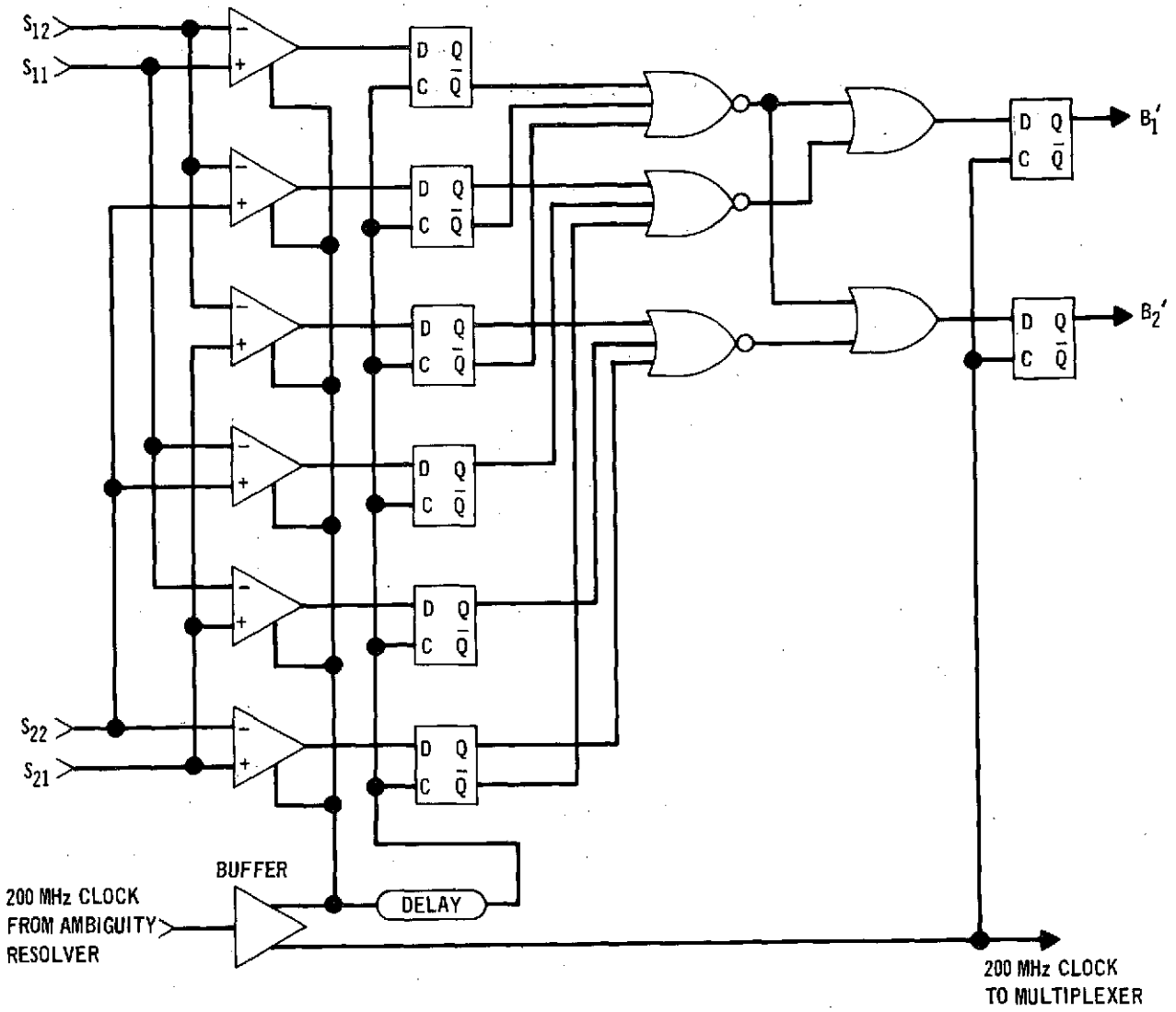

FIGURE 14 PQM DECISION MODULE

is a logic block diagram of the PQM decision module. The four inputs S_{12}, S_{11}, S_{22}, and S_{21} are each compared to one another at the proper time as determined by the 200 MHz strobe to each comparator.

The AM685 integrated comparators were used to make the six comparisons required. Six latching MECL III 500 MHz type D flip-flops were used as the register following the comparators.

The register latched the comparator outputs and thus increased the allowable time for decoding of the detected information. The six comparisons are represented by the following equations:

$$S_{12} \odot S_{11} = C_1$$
$$S_{12} \odot S_{22} = C_2$$
$$S_{12} \odot S_{21} = C_3$$
$$S_{11} \odot S_{22} = C_4$$
$$S_{11} \odot S_{21} = C_5$$
$$S_{22} \odot S_{21} = C_6$$

The logical decisions to determine which input is present can be represented by the equations:

$$S'_{12} = C_1 C_2 C_3$$
$$S'_{11} = \overline{C}_1 C_4 C_5$$
$$S'_{22} = \overline{C}_2 \overline{C}_4 C_6$$
$$S'_{21} = \overline{C}_3 \overline{C}_5 \overline{C}_6$$

Referring to Section 3.1 the truth table for reconstructing the data is seen to be:

	B'_1	B'_2
S'_{11}	0	0
S'_{21}	0	1
S'_{22}	1	0
S'_{12}	1	1

The prime notation is used to indicate detected signals. Using the above truth table the final data reconstruction equations can be written.

$$(S'_{12} + S'_{22}) = B'_1$$
$$(S'_{12} + S'_{21}) = B'_2$$

MECL III "or" and "nor" gates were used for the above logical reconstruction. A pair of type D flip-flops were used to reclock the data before it was sent to the multiplexer module.

PQM Receiver Multiplexer Module

Figure 15 is a logic diagram of the PQM receiver multiplexer module. Multiplexing of B'_1 and B'_2 is accomplished by performing the logical "and" function on B'_1 and C and B'_2 and $\overline{C}$. The logical "or" operation is then performed on the results. The "or" output is reclocked at a 400 MHz rate giving a 400 Mbps NRZ output. The time placement of B'_1 and B'_2 is determined by inserting a one-half period delay in the B'_2 line. This guarantees that B'_1 is placed before B'_2 in the multiplexed data stream. The PQM receiver multiplexer module was implemented with MECL III integrated circuits with the exception of the buffers, which were implemented with discrete components.

PQM Ambiguity Resolver

The PQM ambiguity resolver is used to resolve the 180° phase ambiguity present in the receiver 200 MHz clock. Figure 16 is a logic diagram of the PQM ambiguity resolver. The received data from detector 2 is amplified by an amplifier that has a double ended output. This double ended output is needed so that no external threshold setting is required for the comparison that follows the amplifier. Figure 17 is a timing diagram for the ambiguity resolver. The comparator is strobed with the 400 MHz

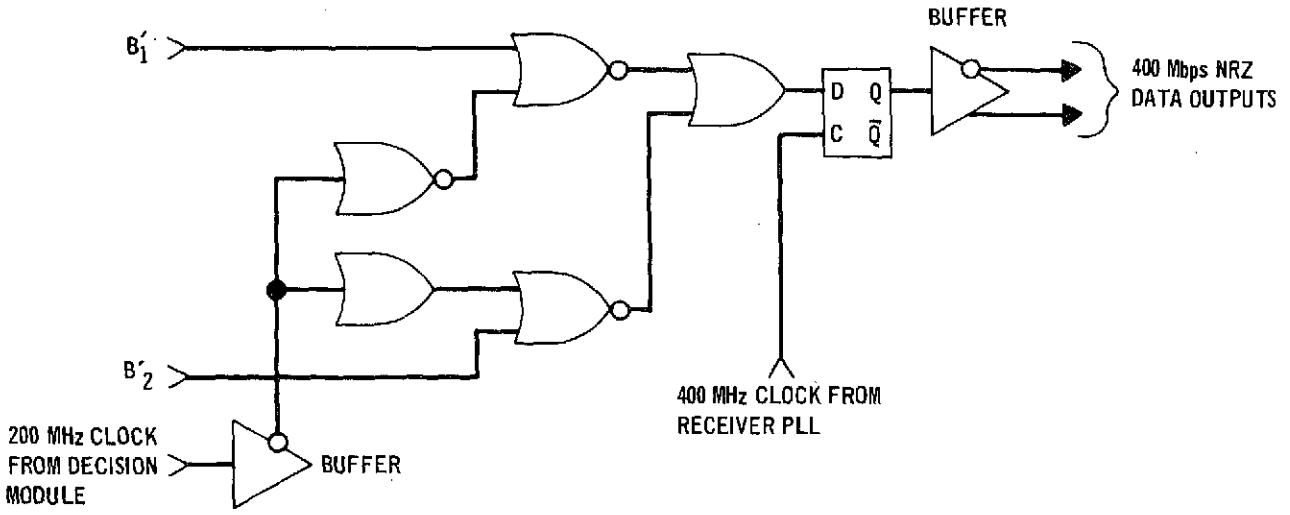

FIGURE 15 PQM RECEIVER MULTIPLEXER MODULE

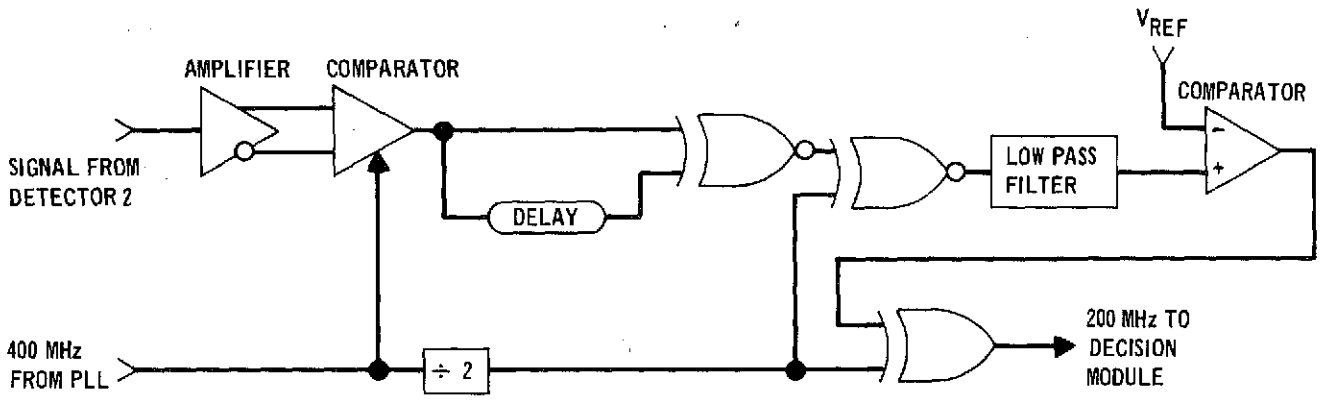

FIGURE 16 PQM AMBIGUITY RESOLVER

clock. The output of the comparator has the form of 400 MHz NRZ type data. By delaying this data by 2.5 ns and performing an "exclusive nor" operation on it and on the undelayed data, a pulse train with pulses spaced at integer multiples of 5 ns is obtained. This pulse train is used for the 200 MHz phase reference. Examples of the "exclusive nor" gate phase comparator output are given in Figure 17 for both phase conditions. The phase comparator output is low pass filtered and compared to a reference voltage level to determine if the 200 MHz clock requires phase correcting.

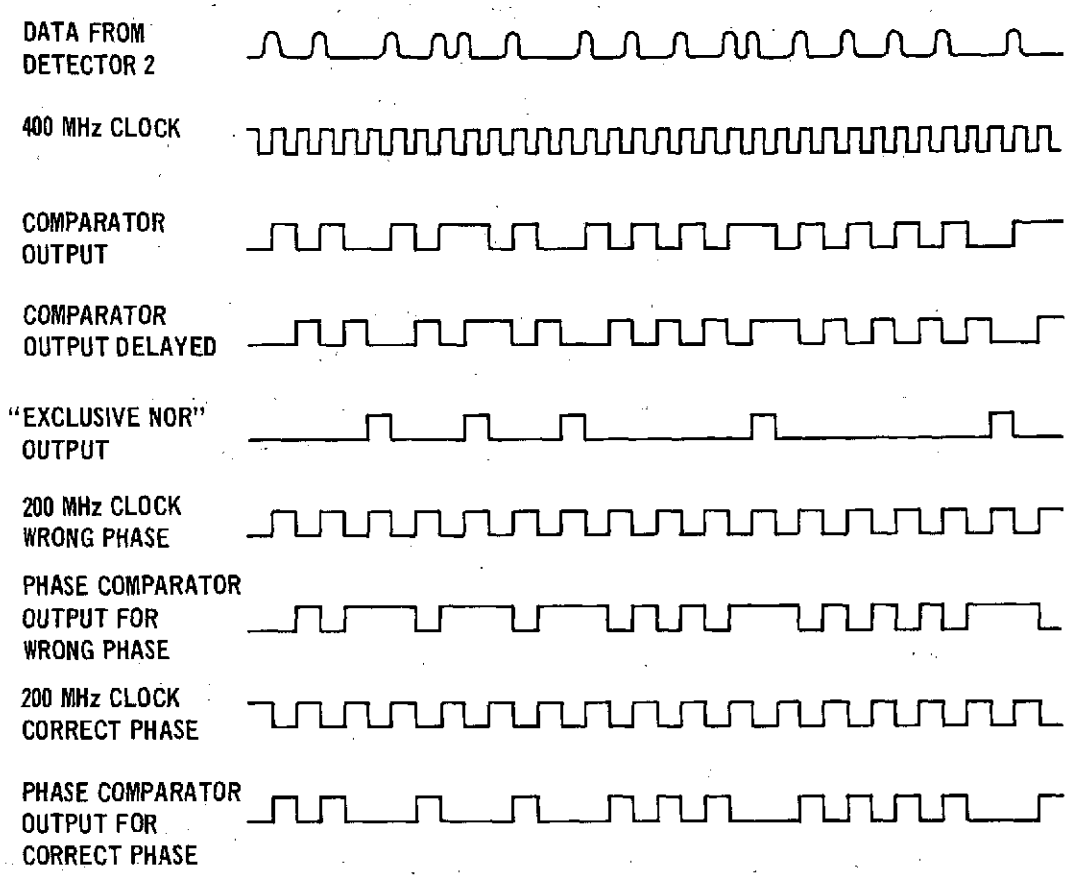

FIGURE 17 PQM AMBIGUITY RESOLVER TIMING DIAGRAM

Phase correcting is accomplished with an "exclusive or" gate. Various limits must be imposed on the received data to insure proper operation of the PQM ambiguity resolver. These limits are not severe and are calculated in the following analysis. Referring to Figure 17 it can be seen that the "exclusive nor" output goes high only when there is a time slot change in the received data pulses. The "exclusive nor" output remains high for one 400 MHz period and then returns low. Time slot change means a delayed pulse followed by a nondelayed pulse, or vice versa. The sample data shown in Figure 17 does not skip any pulses due to them appearing in the opposite polarization. It can be easily seen that for each such missing pulse the "exclusive nor" output would go high and remain high for two 400 MHz periods. Thus when the "exclusive nor" output is compared to the 200 MHz clock in the phase comparator "exclusive nor" gate, the net change in duty

cycle due to each missing pulse is zero. Assume first that the data does not contain any time slot changes. For this case the phase comparator output would have equal duty cycle and thus equal average values for either phase of the 200 MHz clock. The average value of the output voltage for N 400 MHz periods is given by

$$Vave = \frac{V_1 N + V_o N}{2N}$$

where V_1 is equal to the high logic level voltage and V_o is equal to the low logic level voltage of the phase comparator. Now if n time slot changes occur for the N 400 MHz periods the average voltage for one of the clock phases is given by:

$$V_1 ave = \frac{V_1 (N+n) + V_o (N-n)}{2N}$$

and the average voltage for the opposite clock phase is:

$$V_2 ave = \frac{V_1 (N-n) + V_o (N+n)}{2N}$$

The change in the phase comparator output average voltage for the two clock phase conditions is given by:

$$\Delta V = V_1 ave - V_2 ave = \frac{(V_1 - V_o) n}{N}$$

The above equations do not include the effects of rise and fall times but these effects are secondary and are omitted from the analysis.

The minimum number of time slot changes in a given interval is limited by the minimum detectable ΔV. The low speed comparator in the ambiguity resolver was implemented with a LM311 integrated comparator. Using the LM311 a ΔV of 1 mv could be detected. The output swing $(V_1 - V_o)$ of the "exclusive nor" gate used as the phase comparator is 800 mv, thus

$$\frac{\Delta V}{(V_1 - V_o)} = \frac{1 \text{ mv}}{800 \text{ mv}} = \frac{n}{N} = 1.25 \times 10^{-3}.$$

Now, if n = 1, we have

$$\frac{1}{N} = 1.25 \times 10^{-3}$$

or

$$N = 800$$

thus the data must have one time slot change for every 800 400 MHz periods or in other words one time slot change in every 800 bits. In order to recognize what causes a time slot change in the data refer to the encoding truth table from Section 3.1 which is repeated here for convenience.

	B_1	B_2
S_{11}	0	0
S_{21}	0	1
S_{22}	1	0
S_{12}	1	1

The following conditions are time slot changes:

$S_{11} \longrightarrow S_{12}$
$S_{12} \longrightarrow S_{11}$
} polarization 1

$S_{21} \longrightarrow S_{22}$
$S_{22} \longrightarrow S_{21}$
} polarization 2

These correspond to the following data blocks:

00,0,2,4, ... , 1 1
11,0,2,4, ... , 0 0
} polarization 1

01,0,2,3, ... , 1 0
10,0,2,4, ... , 0 1
} polarization 2

The data block table above indicates that any number of 2 bit PQM words from the opposite polarization can appear between the time slot change words. The ambiguity resolver uses only one polarization but either one can be used. From the above analysis it can be seen that the data limits imposed for proper operation of the ambiguity resolver are not severe.

Referring to Figure 16 the amplifier, 400 MHz comparator, "exclusive nor" gates, and "exclusive or" gate were fabricated with discrete components. The divide by 2 function and the low frequency comparator were implemented with a MECL III 500 MHz flip-flop and a LM311 respectively.

3.1.6 400 MHz Phase Locked Loop. The 400 MHz Phase Locked Loop (PLL) is used to generate a 400 MHz clock source for the receiver. It recovers the 400 MHz component from the S_1 portion of the received signal and generates a continuous signal which is synchronized with the input pulses. The intervals between pulses are integer multiples of 2.5 ns. Thus each pulse can be compared to the PLL generated 400 MHz signal (whose period is 2.5 ns). The PLL uses this comparison to form the generated signal which is properly aligned timewise with the input pulses.

The block diagram of the 400 MHz PLL is shown in Figure 18. The input pulse train from detector 1 is amplified and filtered in the preamplifier module to obtain its 400 MHz component for comparison with the internally generated 400 MHz signal. The internal 400 MHz signal is developed by frequency multiplication of the 100 MHz output of the VCXO (Voltage Controlled Crystal Oscillator). This 400 MHz signal is distributed to the output and the phase comparator. The output of the phase comparator is a signal representative of time error between the internal 400 MHz signal and the input pulse train. This error signal is shaped by the active filter and is used to tune the VCXO, causing the 400 MHz signal to track the received pulse train.

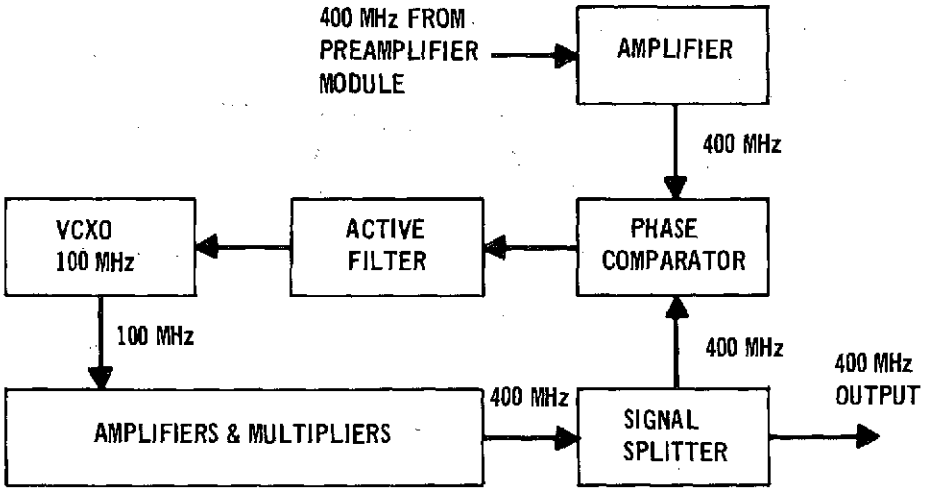

FIGURE 18 BLOCK DIAGRAM – 400 MHz PHASE LOCKED LOOP

The PLL bandwidth was selected to provide minimum acquisition time while maintaining proper timing during the normal intervals in which no pulses were present in S_1. Similarly the acquisition bandwidth was maximized within the above constraints.

3.2 EXISTING EQUIPMENT. The components coded as "existing equipment" in Figure 3 were previously developed and fabricated by MDAC-E for various IRAD programs over the past few years. These components were made available for the Wideband PQM program.

3.2.1 200 MHz Mode Locked Laser. Figure 19 is a block diagram of the 200 MHz Mode Locked Laser used in this program. It consists of an optically pumped, water cooled Nd:YAG laser rod, an acousto-optic mode-locker and two reflectors spaced 75 cm optical path length apart. The mode-locker is a quartz block, cut to the Brewster angle, with the acousto-optic transducer bonded to it. The transducer is resonant at ~100 MHz, the exact operating frequency is adjusted by temperature tuning the acoustic length of the quartz block mounted in an oven. One reflector has maximum reflectivity at the laser's operating wavelength of 1.06 μm and the other has ~1.5% transmission for coupling out the optical pulses.

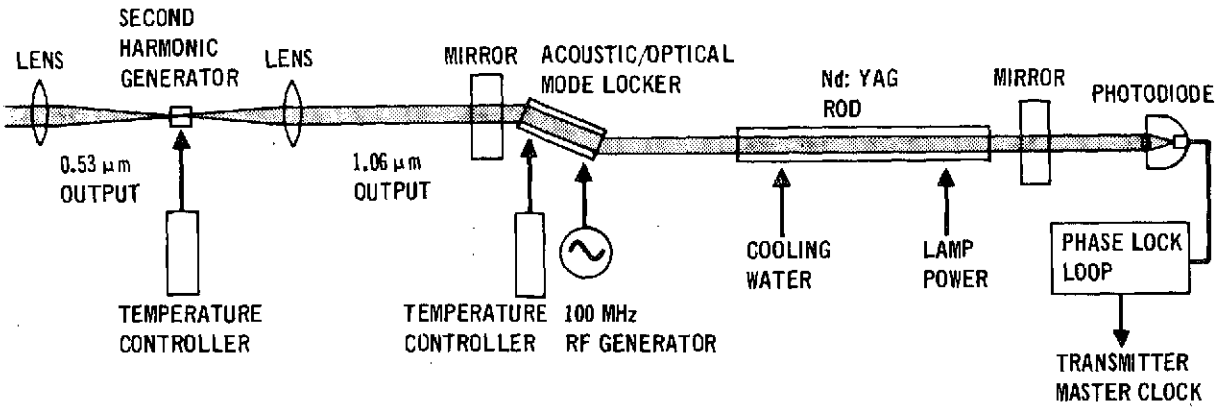

FIGURE 19 200 MHz MODE LOCKED FREQUENCY DOUBLED Nd: YAG LASER

The output is a train of pulses at a 200 MHz rate at 250 mW average power. The pulse width is ~225 ps at the 10% amplitude points with an amplitude stability of ±4% peak to peak. External second harmonic generation was chosen over internal to obtain extremely short pulse duration (~160 ps) at a lower (3 - 5 mW) power level at the 0.53 μm wavelengths. The barium sodium niobate crystal used for frequency doubling is maintained at its phase matching temperature in a controlled oven.

Figure 20 shows the 0.53 μm laser pulse output. The photodiode used for detecting these pulses has a 70 ps risetime. Referring to the photographs in Figure 20 it is seen that the pulse width is approximately ~200 ps at the base.

3.2.2 200 MHz Phase Locked Loop. The transmitter master clock is derived from the mode locked laser output signal rather than from the reference oscillator which drives the laser mode locking element in order to eliminate the effect of phase shifts which occur between the laser output and the mode locker drive signal. These phase shifts invariably accompany laser cavity length detuning from the mode locking center frequency due to thermal effects.

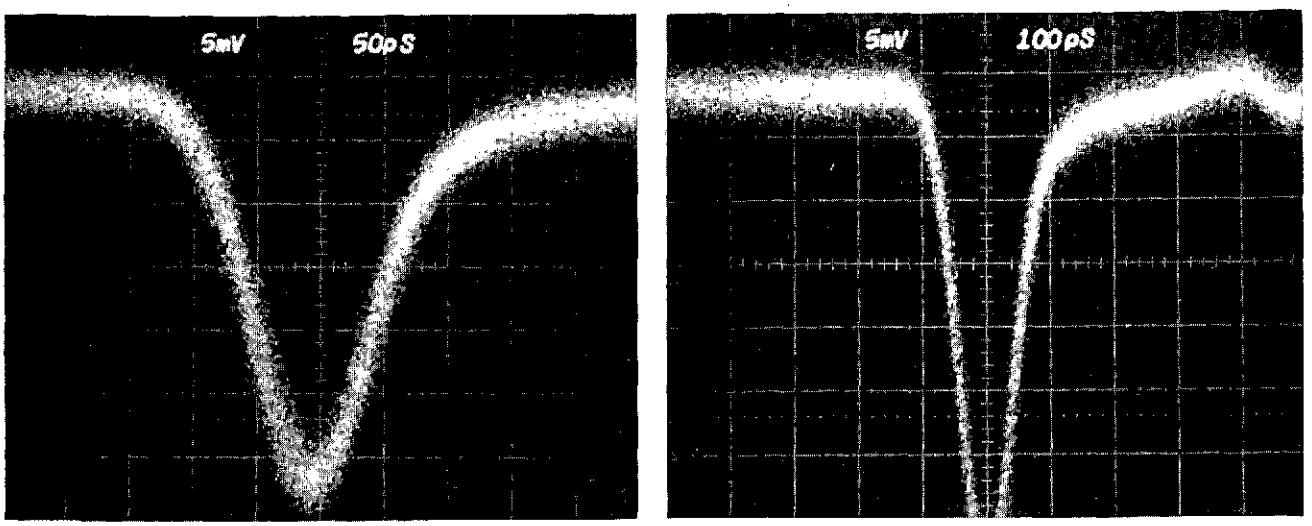

FIGURE 20 0.53 μm LASER PULSE OUTPUT

A high speed photodiode detector is used to detect a sample of the 1.06 μm laser output as shown in Figure 19. A stable 100 MHz VCXO and frequency multiplier chain are then phase locked to the detected laser signal. The phase locked loop provides narrow band filtering as well as amplitude stable output signals at 200 MHz and 400 MHz as required by the transmitter electronics.

3.2.3 Optical Modulators. The two electrooptical modulators that were used for this program were both of the single pass variety. Modulator 1 used two crystals in series optically and in parallel electrically with a single matching network and single drive signal. This modulator required 28 volts for full half-wave switching. The worst case dynamic extinction ratio of this modulator was measured at 30 to 1. Modulator 2 used two crystals in series optically with separate matching networks and separate identical drive signals. This separate matching technique was used to decrease the reflection coefficient seen by the modulator driver. The second modulator in this system required a 400 Mbps response while the first modulator only required a 200 Mbps

REPRODUCIBILITY OF THE ORIGINAL PAGE IS POOR

response. Modulator 2 required 22.5 volts for full half-wave switching. Its worst case dynamic extinction ratio was measured to be 20 to 1. Optical transmission for both modulators was measured at approximately 75% each. Figure 21 shows photographs of PQM encoded laser pulses. A 400 Mbps 63 bit sequence PN code was used as the encoding data source and a high speed silicon avalanche photodiode was used as the detector for these photographs.

3.3 NASA FURNISHED EQUIPMENT. The following equipment was furnished by NASA for use on this contract:

1. 400 Mbps PN generator
2. 400 Mbps error rate electronics
3. Dynamic Cross Field Photomultiplier

3.3.1 400 Mbps PN Generator. The 400 Mbps PN generator was used as the data source during system testing of the 400 Mbps PQM system. This generator is capable of generating PN codes with sequence lengths of 31, 63, 127, 511, or 1023 bit. Most of the system tests utilized a 63 bit sequence code.

3.3.2 400 Mbps Error Rate Electronics. The 400 Mbps error rate electronics are capable of generating an internal reference PN code and comparing it bit by bit to a received PN code which has been processed over the laser communication link. The error rate electronics are compatible with the 400 Mbps PN generator codes.

3.3.3 Dynamic Cross Field Photomultipliers. It was decided, after testing various static cross field photomultipliers, that dynamic cross field photomultipliers would be used as detectors in this program. The static tubes tested had noise figures from 7 dB to 8 dB, nonuniform cathode response, nonuniform gains, and in general low gains. The two DCFP's used were delivered to NASA by MDAC-E under contract NAS5-11471 and returned to MDAC-E as GFE equipment for this program. Their noise figures were measured at 0.44 dB and 1.7 dB for DCFP S/N 013 and S/N 027 respectively.

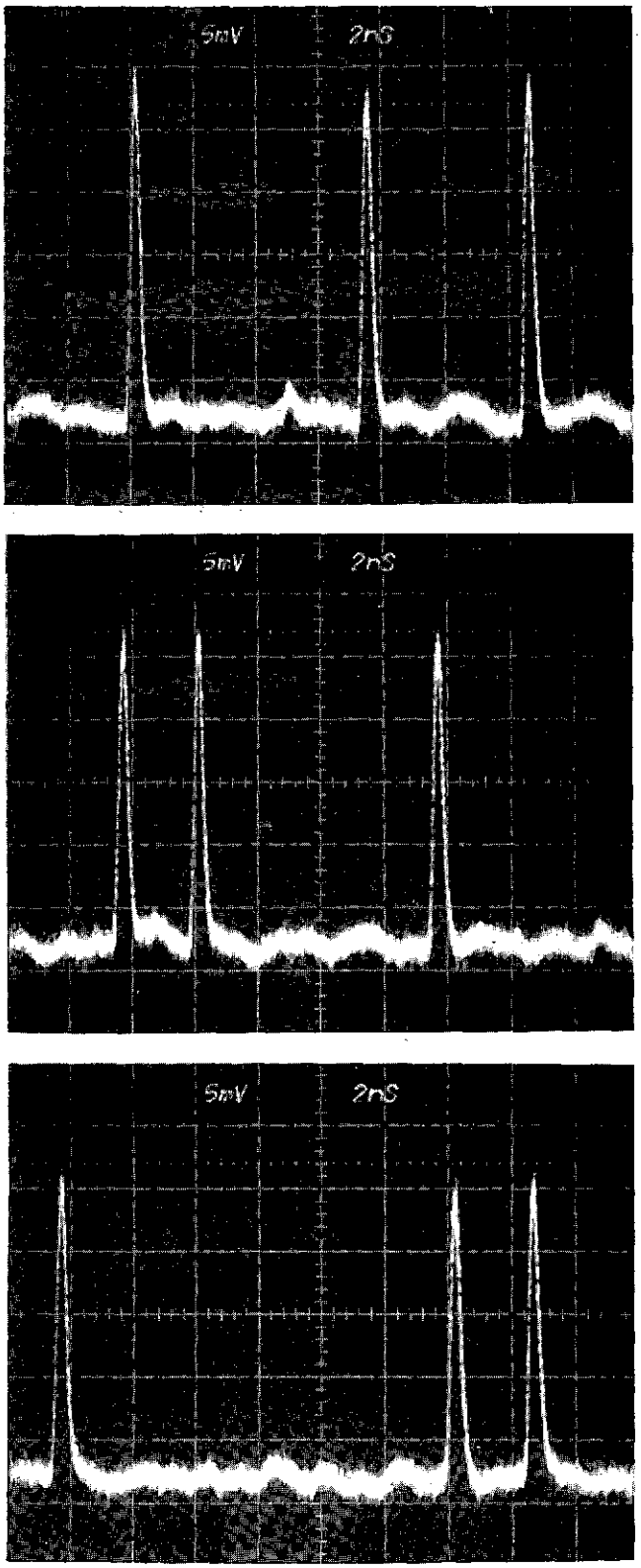

Portions of a PQM Modulated Test Sequence. Polarization P1 used for these Photographs

REPRODUCIBILITY OF THE ORIGINAL PAGE IS POOR

FIGURE 21 PQM MODULATED LASER SIGNAL

The detector electronics, which include the RF drive and sync circuits for single DCFP operation, were also used at MDAC-E as GFE equipment. The detector electronics were modified to include several recent design changes which allow improved performance at the lower operating currents desired for DCFP S/N 027. Figure 22 is a block diagram of the dual detector synchronization scheme used in the PQM setup. DCFP S/N 027 was operated with the detector electronics in the AGC mode with internal synchronization. DCFP S/N 013 was operated with separate dc power supply and RF drive chain. The RF drive chain for DCFP S/N 013 was phase locked to a sample of the output of the detector electronics to provide synchronization for the second receiver. AGC was not provided for the second receiver. Each receiver was set up to receive one polarization of the input PQM signal.

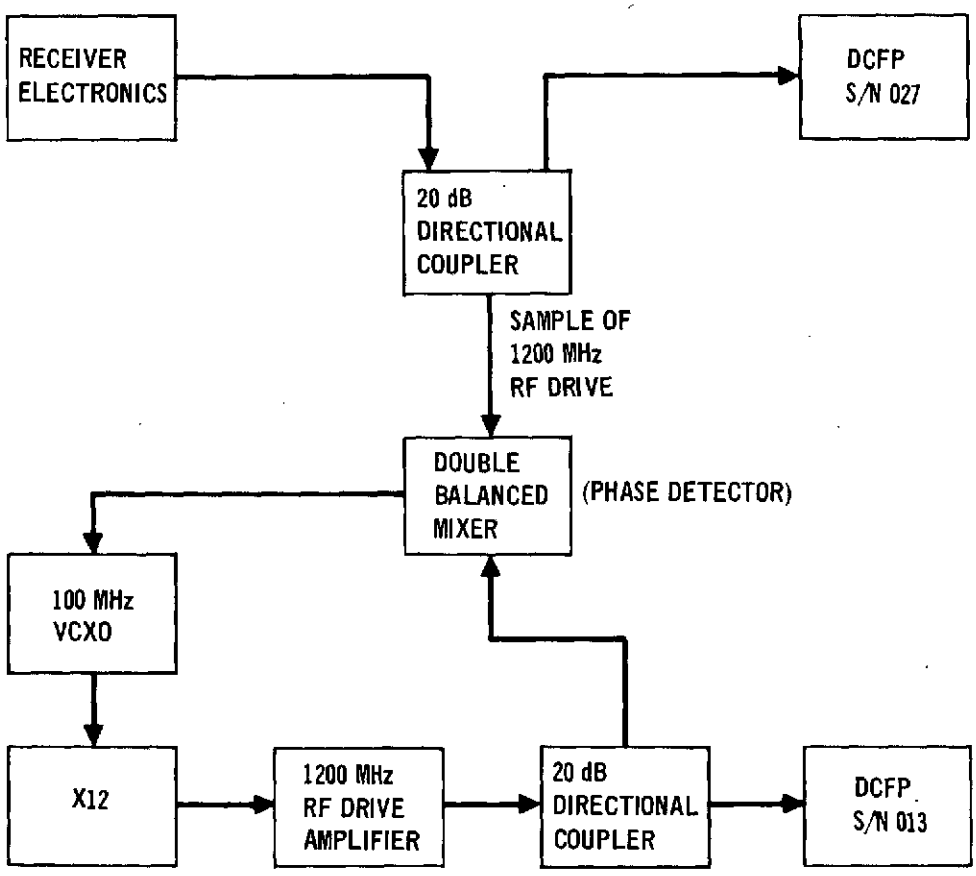

FIGURE 22 DUAL RECEIVER SYNCHRONIZATION SCHEME

4. PERFORMANCE TESTS

4.1 GAUSSIAN NOISE TESTS. Prior to complete system integration, the wideband PQM electronics were integrated and tested using the PQM Data Simulator with additive Gaussian noise. These tests were designed to allow the complete electronics package to be tested under a signal plus noise condition and to assist in trouble shooting of the electronic components. Figure 23 is a block diagram of the PQM electronics package and Gaussian noise source. Gaussian noise was added to the simulated output by using attenuators and wideband amplifiers as shown in Figure 23. The output of the PQM Data Simulator was attenuated to a level such that the ratio of the simulated pulse amplitude and the RMS noise of the amplifier was in a range of interest. The attenuator at the amplifier output was then set for proper pulse amplitude at the receiver front end. Various signal-to-noise ratios were then obtained by either increasing or decreasing the input attenuator and changing the output attenuator by an equal amount so as to offset any overall gain changes.

Initial bit error rate (BER) tests using Gaussian noise indicated that we were 10 dB worse than theoretical at 10^{-6} bit error rate. By making use of bit blanking techniques which allow us to localize bits with high error rates, it was determined that clock feedthrough on one of the four signal lines to the decision module was causing the degradation. The feedthrough was traced to two parallel strip-line transmission lines. The problem was corrected and BER tests repeated. Figure 24 shows the results of these tests. In Figure 24 we have plotted signal-to-noise ratio (SNR) = $20 \log_{10} A/\sigma$ versus bit error rate, where A is the signal pulse voltage amplitude and σ is the RMS noise voltage. At 10^{-6} bit error rates the system was seen to be 1.7 dB worst than theoretical. We felt these results showed that the electronics were operating close enough to theoretical such that they could be used in the system with minimum degradation.

4.2 SYSTEM BER TESTS. Figure 25 and 26 are photographs of the laboratory setup for the wideband PQM system. Figure 25 shows the PQM transmitter setup and Figure 26 shows the PQM receiver setup. As can be seen in the

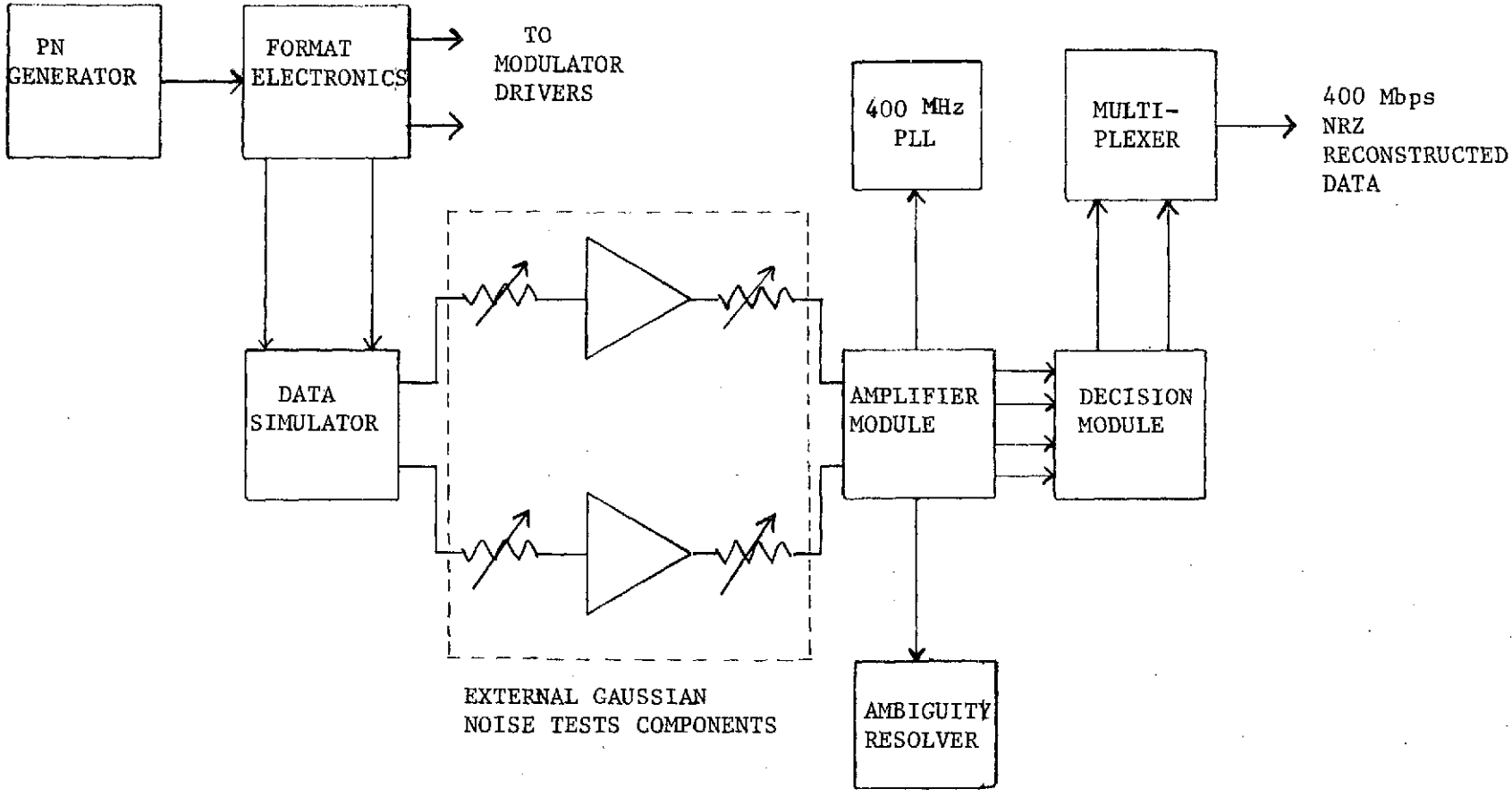

FIGURE 23 400 Mbps PQM ELECTRONICS BLOCK DIAGRAM

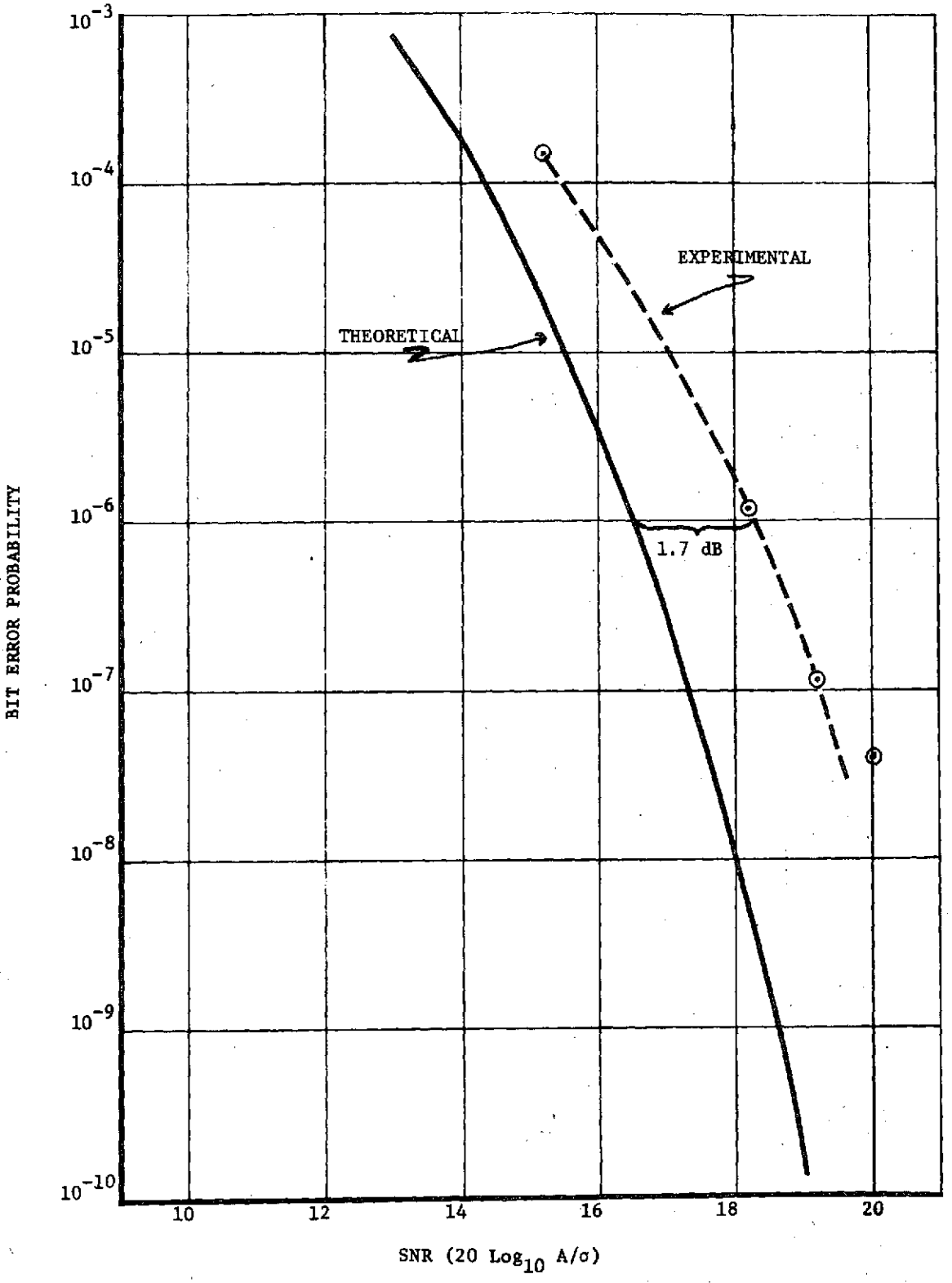

FIGURE 24 PQM ERROR PROBABILITY WITH CONSTANT AMPLITUDE PULSES AND GAUSSIAN NOISE

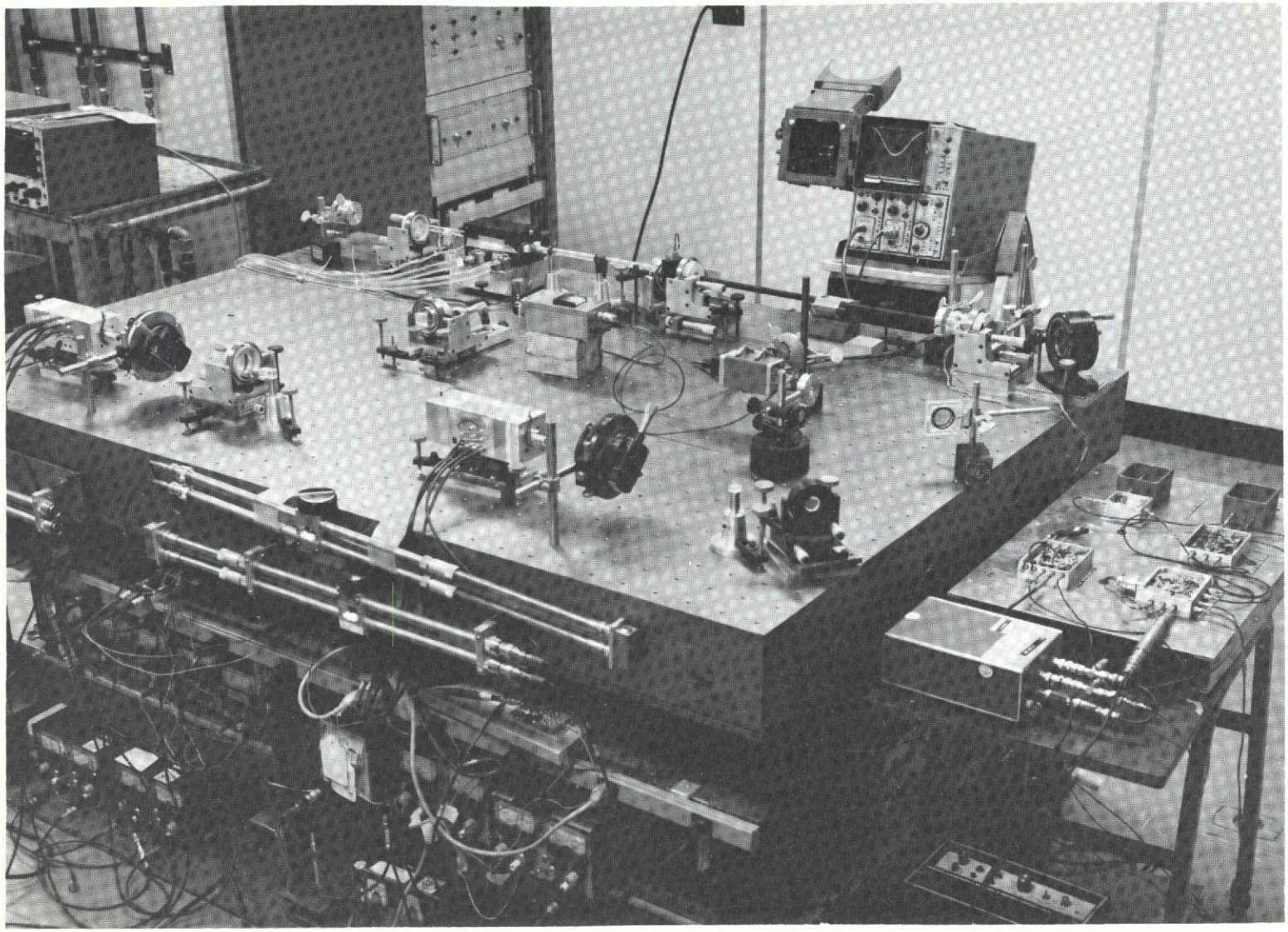

FIGURE 25 PHOTOGRAPHS OF 400 Mbps PQM TRANSMITTER SETUP

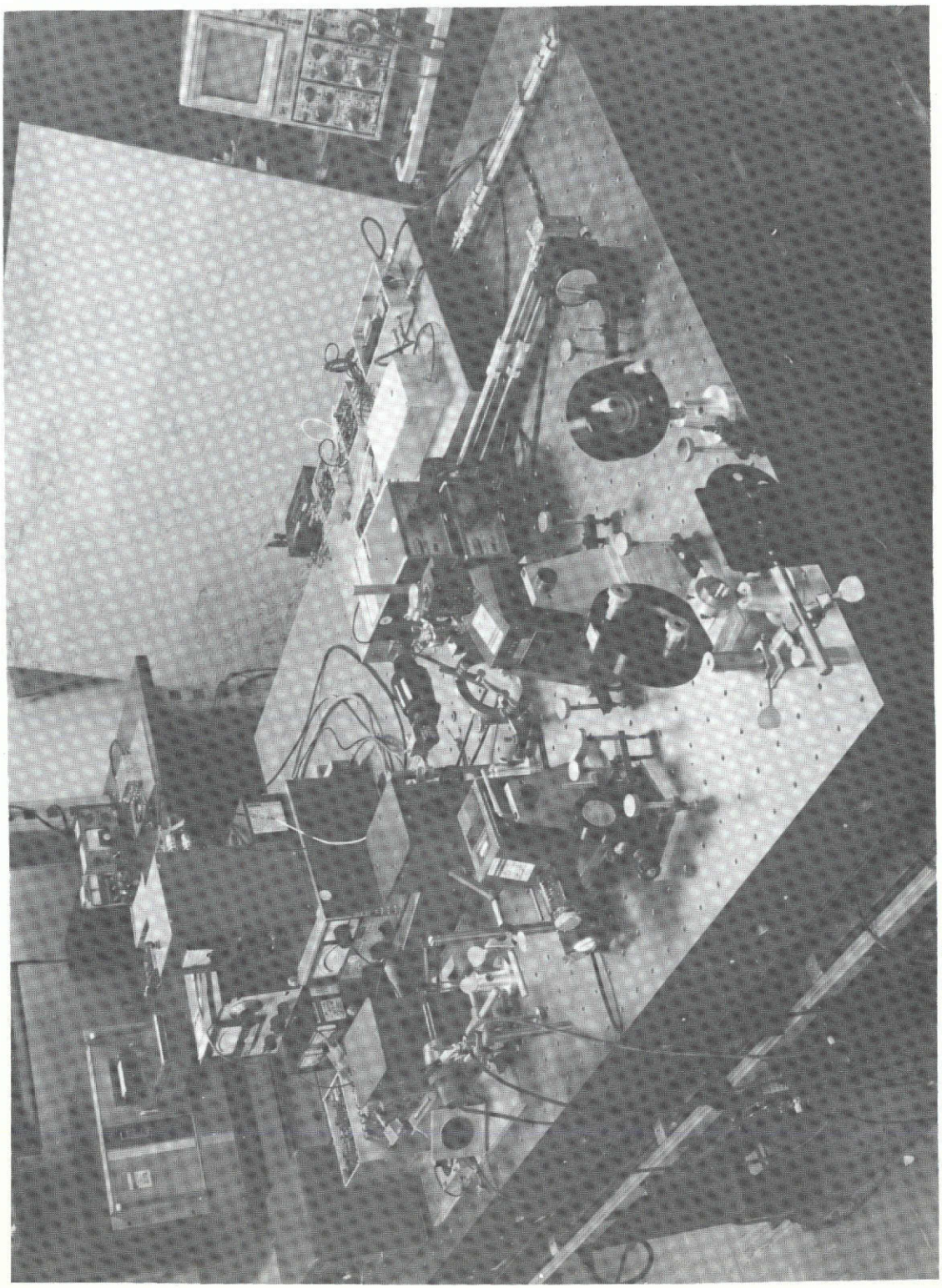

FIGURE 26 PHOTOGRAPH OF 400 Mbps PQM RECEIVER SETUP

REPRODUCIBILITY OF THE
ORIGINAL PAGE IS POOR

photographs separate optical benches were used for the receiver and transmitter setups. These benches were spaced approximately 15 feet apart and required no electrical connections between them during system bit error rate tests.

4.2.1 Comparison of PQM and PGBM. One of the requirements of this contract was to compare PGBM BER data obtained during NASA contracts NAS5-11471 and NAS5-11474 to PQM BER data obtained during this contract. The best PGBM BER data on record from those contracts was for an extinction ratio of 10 to 1. In order to make a direct comparison between the two modulation schemes it was decided to compare PQM with an extinction ratio of 10 to 1 to the previously obtained PGBM data. In Figure 27, which shows this comparison, the bit error probability is plotted against mean signal photoelectrons per bit referred to the transmitter. The referral to the transmitter is necessary in order that the true power advantage be explicit on the graphical comparison. If the mean signal photoelectrons per bit were not referred to the transmitter the 3 dB advantage obtained by transmitting all of the laser pulses in the PQM format would not be explicit in graphical representations. Referring to Figure 27 the two theoretical curves for PQM and PGBM are seen to differ by 5.4 dB at 10^{-6} bit error rate. The two experimental curves differ by 6.8 dB at 10^{-6} bit error rate. The 6.8 dB difference encompasses approximately a 2 dB improvement over the modulation format predictions. This 2 dB is due to state of the art improvements in various system components during the interim between the two tests.

4.2.2 PQM BER Tests Without Background. The best results obtained during system tests seemed to be limited by the modulator extinction ratio. The best modulator extinction ratio obtained was approximately 20 to 1. Figure 28 shows a portion of the PQM encoded test code used for BER tests. This particular portion of the test sequence contained the worst extinction ratio observed in the test sequence. In PQM there are four possible conditions for each decision made.

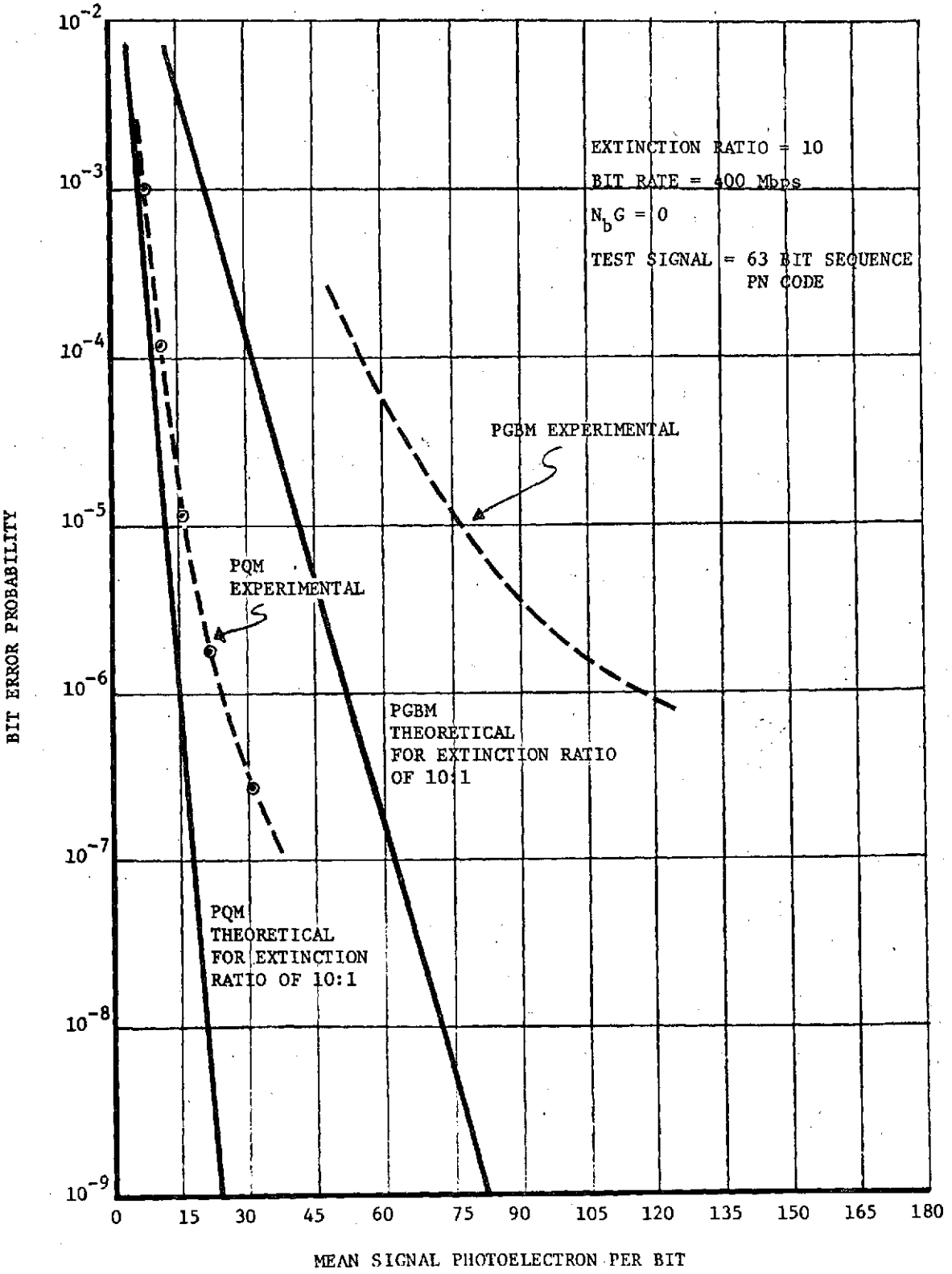

FIGURE 27 COMPARISON OF PQM AND PGBM MODULATION FORMATS

FIGURE 28 PHOTODIODE OUTPUTS OF PQM ENCODED TEST SIGNAL

These are:

P_1 undelayed $\longrightarrow S_{11}$

P_1 delayed $\longrightarrow S_{12}$

P_2 undelayed $\longrightarrow S_{21}$

P_2 delayed $\longrightarrow S_{22}$

REPRODUCIBILITY OF THE
ORIGINAL PAGE IS POOR

Worst case extinction ratio for PQM is defined as the ratio of the condition with the greatest mean rate to the condition with the second greatest mean rate within a given decision interval. Referring to Figure 28 several cases can be found where the extinction ratio is no better than 20 to 1. Below each polarization is a plot of baseline noise for the avalanche photodiode used as the detector. This baseline noise should be subtracted from the signal plus baseline noise plot when calculating extinction ratio. The signal plots shown in Figure 28 were obtained by using an x-y plotter in conjunction with a sampling oscilloscope. Using this technique many more samples per time interval can be obtained than with a sampling oscilloscope alone. Thus a more accurate description of a waveform is obtained.

Using the same technique as in Figure 28, Figure 29 shows the two DCFP outputs for the same portion of the test sequence. The slightly different pulse shapes and baseline ringing are integrated out in the PQM preamplifier module. The apparent amplitude descrepancy is also compensated for in the PQM preamplifier module.

Figure 30 is a strip chart recording representative of the laser stability during the BER tests. It shows the 1.06 μm amplitude stability using three different chart speeds; 20 s/cm, 2 s/cm and 0.2 s/cm. The recorder used has flat response up to 60 Hz and is 6 dB down at 120 KHz. The optical power meter has flat frequency response to 20 KHz. In Figure 30b the beam was interrupted to show that the zero level is at the bottom of the scale. Peak amplitude variation is seen to be $\pm 4\%$. A high bandwidth real time oscilloscope was also used to check for relaxation oscillations, none were observed during the BER test intervals or at any time when the laser was properly adjusted.

Figure 31 is a bit error rate plot for an extinction ratio of 20 to 1. The background for this case was zero. From Figure 31 it is seen that the experimental results are 2.05 dB off theoretical

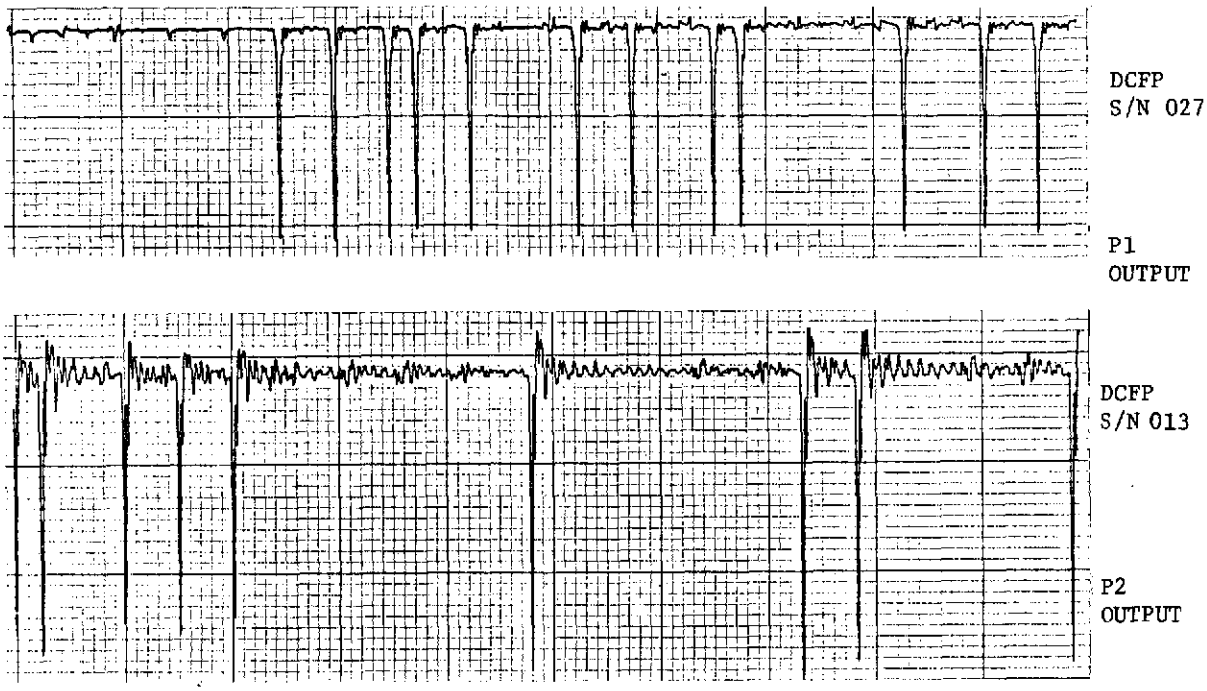

FIGURE 29 DCFP OUTPUTS OF PQM ENCODED TEST SIGNALS

at 10^{-6} bit error rate. The mean signal photoelectrons per bit at 10^{-6} is seen to be 17.

4.2.3 PQM BER Tests With Background. Background illumination for BER measurements was implemented using a dc powered incandescent lamp behind a small pinhole. An appropriate lens was used to image the pinhole to a circular spot about 0.4mm diameter on the cathode. Background and signal beams were combined using a pellicle beam-splitter. The background signal spot was visually centered on the laser signal spot of the photocathode. Spatial gating of the background was negligible due to the small spot sized used. Referring to Figure 26 which is a photograph of the receiver setup the background sources are seen in place. The incandescent lamp holders can be seen just to the left of center on the photo. The imaging lens and pinhole for each lamp is mounted in the tube protruding from each holder. Background

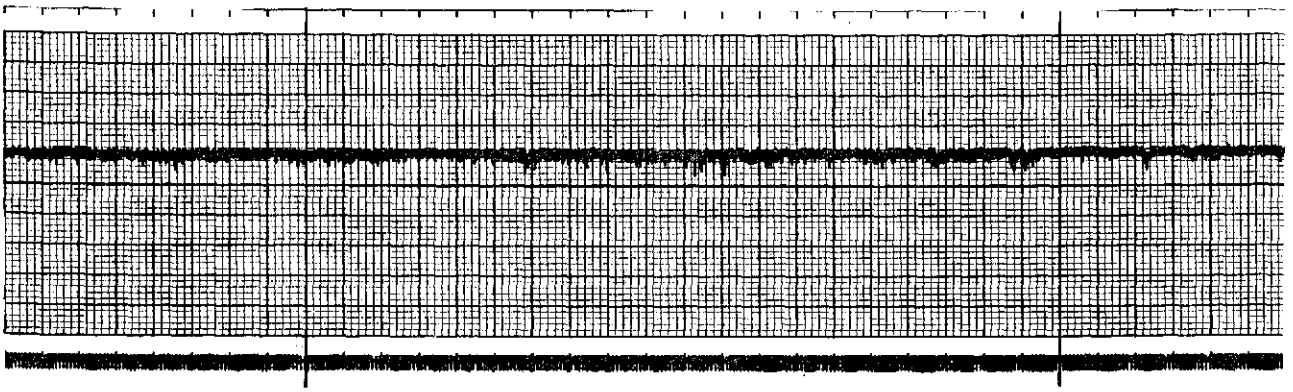

(a) 20 sec/cm

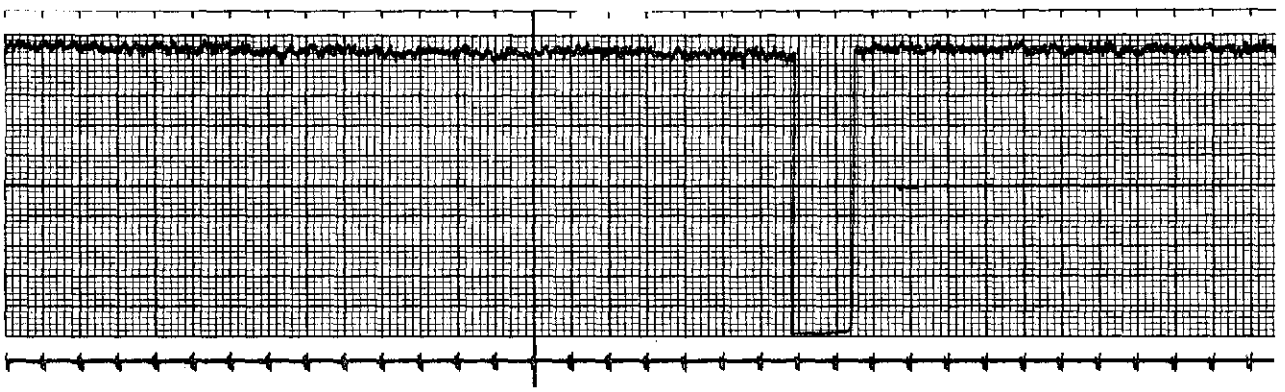

(b) 2 sec/cm

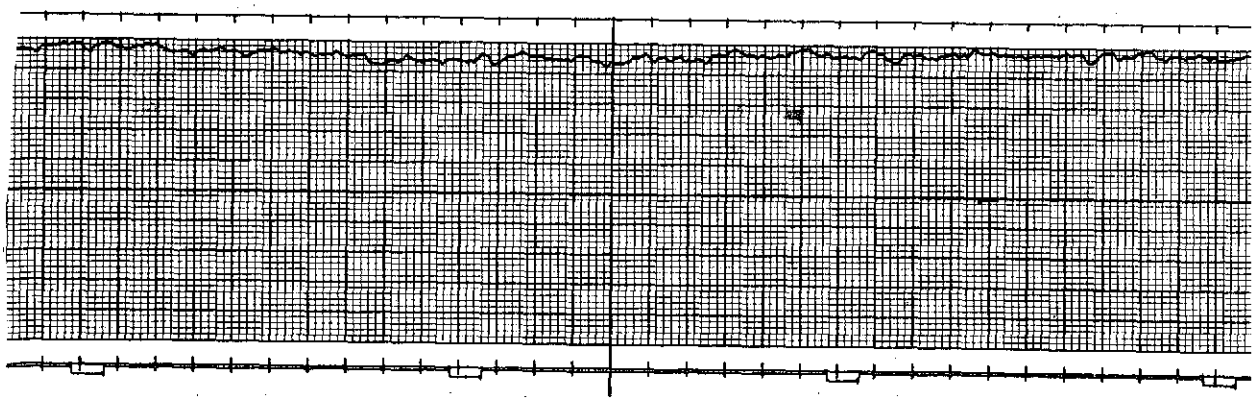

(c) 0.2 sec/cm

FIGURE 30 200 Mpps LASER STABILITY TEST RESULTS

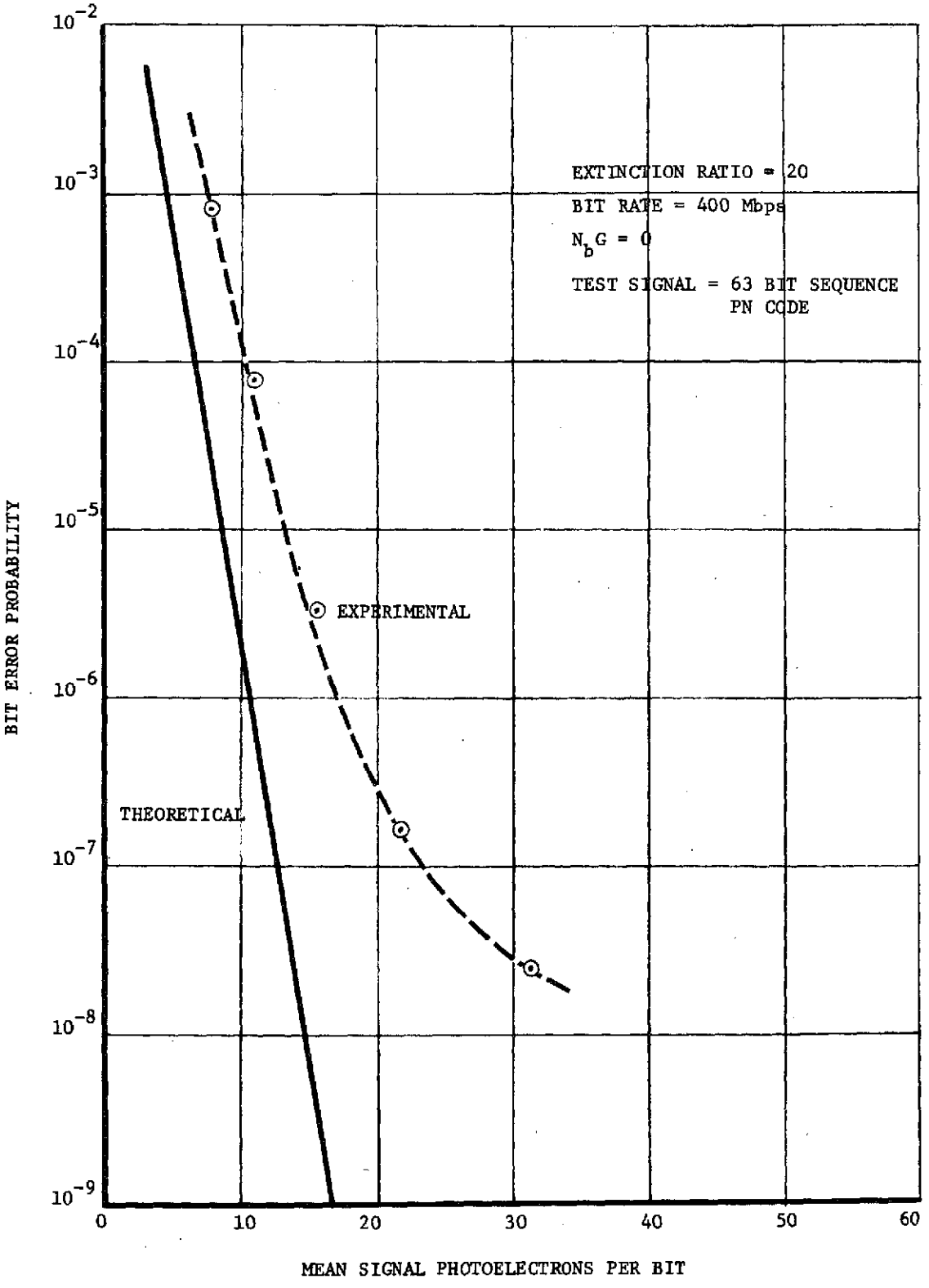

FIGURE 31 PQM BIT ERROR PROBABILITY AS A FUNCTION OF RECEIVED PHOTOELECTRONS PER BIT

levels of 1 pe/ns were set at each DCFP photocathode. The gate widths of the DCFP's were estimated at about 400 ps. However, there are three actual periods for each apparent 400 Mbps PQM gate period. This occurs because the RF drive to the DCFP's is 1200 MHz. Thus the effective 400 MHz gate width is 1.2 ns and $N_b G = 1.20$ pe. Figure 32 shows the results of the BER tests using $N_b G = 1.20$ compared to the theoretically calculated results. From Figure 32 it is seen that the experimental results are 1.76 dB off theoratical at 10^{-6} bit error rate.

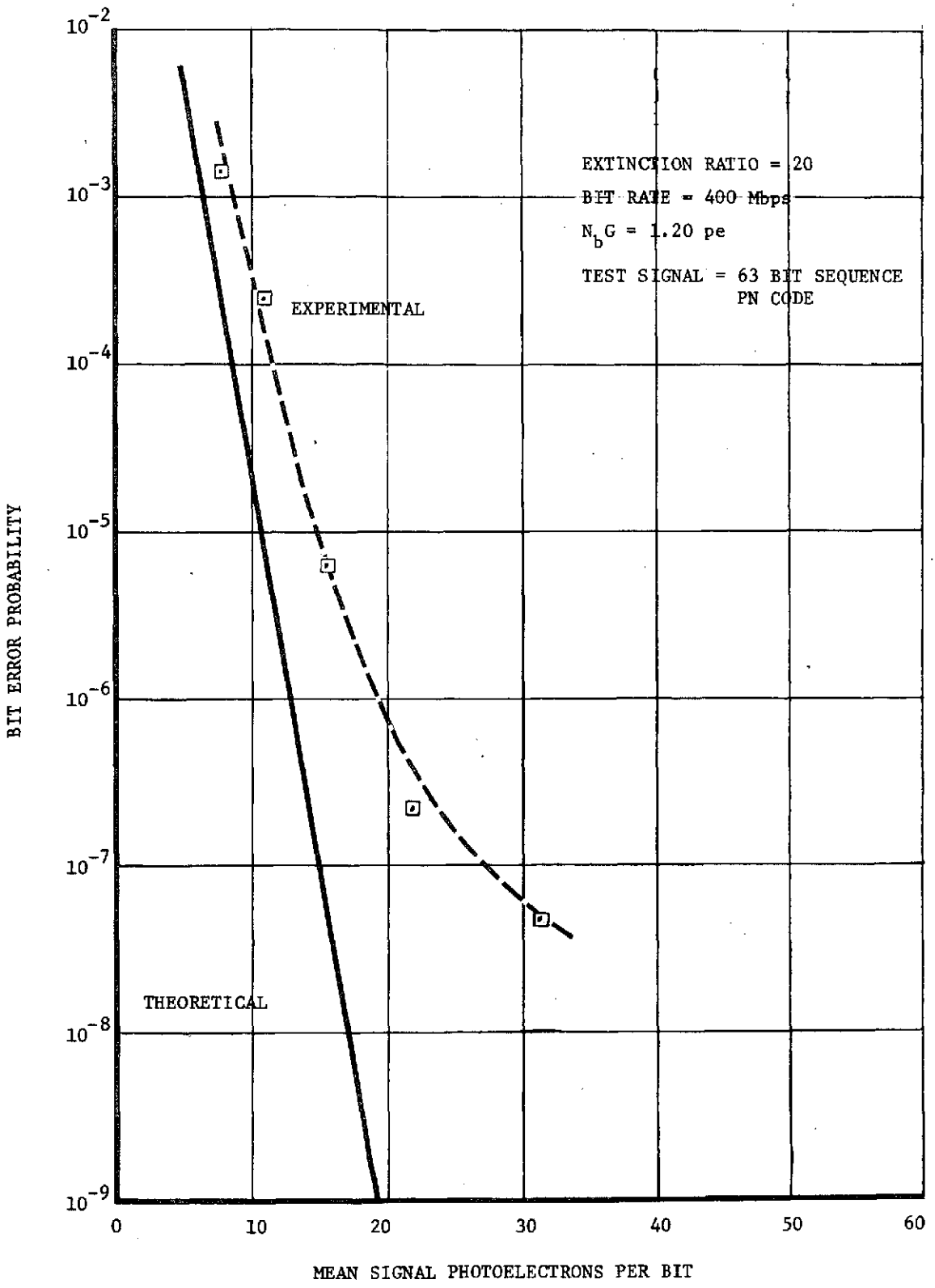

FIGURE 32 PQM BIT ERROR PROBABILITY AS A FUNCTION OF RECEIVED PHOTOELECTRONS PER BIT

5. CONCLUSIONS

During this program, the first 400 Mbps PQM laser communications system was successfully integrated, tested, and demonstrated in the laboratory. The bit error rate tests performed on this system showed approximately 2 dB degradation from the theoretically predicted results. The tests thus confirmed that the theoretical analysis of PQM was valid and that system hardware to implement the PQM modulation format for digital baseband laser communications was practical. A comparison of the PQM test results obtained during this program with PGBM test results from earlier programs confirm the validity of a 5 dB power advantage for the PQM digital baseband laser communication system. The relative ease with which the entire PQM laboratory system was integrated, coupled with the excellent test results achieved with the experimental hardware, demonstrates that PQM is a viable candidate modulation format for an operational 400 Mbps laser communication system.

THIS PAGE INTENTIONALLY LEFT BLANK